The wet deposition of the inorganic ions in the 320 cities across China: spatiotemporal variation, source apportionment, and dominant factors

Rui Li[a], Lulu Cui[a], Yilong Zhao[a], Ziyu Zhang[a], Tianming Sun[a], Junlin Li[a], Wenhui Zhou[a], Ya Meng[a], Kan Huang[a], Hongbo Fu[a,b,c *]

[a] *Shanghai Key Laboratory of Atmospheric Particle Pollution and Prevention, Department of Environmental Science & Engineering, Institute of Atmospheric Sciences, Fudan University, Shanghai, 200433, P.R. China*

[b] *Shanghai Institute of Pollution Control and Ecological Security, Shanghai 200092, P.R. China*

[c] *Collaborative Innovation Center of Atmospheric Environment and Equipment Technology (CICAEET), Nanjing University of Information Science and Technology, Nanjing 210044, P.R. China*

Corresponding author

fuhb@fudan.edu.cn

Abstract

The acid deposition has been considered to be a severe environmental issue in China. The pH, electrical conductivity (EC), and the concentrations of the water soluble ions (NO_3^-, Cl^-, Ca^{2+}, K^+, F^-, NH_4^+, Mg^{2+}, SO_4^{2-}, and Na^+) in the precipitation samples collected from the 320 cities during 2011-2016 across the whole China were measured. The mean concentrations of F^-, NO_3^- and SO_4^{2-} were in the order of winter (6.10, 19.44 and 45.74 μeq/L) > spring (3.45, 13.83, and 42.61 μeq/L) > autumn (2.67, 9.73, and 28.85 μeq/L) > summer (2.04, 7.66, and 19.26 μeq/L). The secondary ions (SO_4^{2-}, NO_3^- and NH_4^+), and F^- peaked in Yangtze River Delta (YRD) and Sichuan basin (SB). The

crustal ions (i.e., Ca^{2+}, Mg^{2+}), Na^{+}, and Cl^{-} showed the highest concentrations in the semi-arid regions and the coastal cities, respectively. The statistical methods confirmed that the mean anthropogenic contribution ratios to SO_4^{2-}, F^{-}, NO_3^{-}, and NH_4^{+} at a national scale were 46.12%, 71.02%, 79.10%, and 82.40%, respectively. However, Mg^{2+} (70.51%), K^{+} (77.44%), and Ca^{2+} (82.17%) were mostly originated from the crustal source. Both Na^{+} (70.54%) and Cl^{-} (60.42%) were closely linked to the sea-salt aerosols. On the basis of the stepwise regression (SR) analysis, it was proposed that most of the secondary ions and F^{-} were closely related to gross industrial production (GIP), total energy consumption (TEC), vehicle ownership, and N fertilizer use, but the crustal ions (Ca^{2+} and K^{+}) were mainly controlled by the dust events. The influence of dust days, air temperature, and wind speed on ions increased from Southeast China (SEC) to Central China, and then to Northwest China (NWC), whereas the influence of socioeconomic factors on acid ions (SO_4^{2-} and NO_3^{-}) displayed the higher value in East China.

Keywords: Water-soluble ions; precipitation; spatiotemporal variation; source identification; China

1. Introduction

Atmospheric wet deposition generally removes efficiently the aerosol particles and dissolved gaseous pollutants from the atmosphere (Garland, 1978; Al-Khashman, 2005; Migliavacca et al., 2005). However, in some regions with severe air pollution, the scavenging of substantial aerosol particles alters the chemical compositions of precipitation and even aggravates the acid deposition (Kuang et al., 2016). Some inorganic ions (i.e., SO_4^{2-}, NO_3^{-}, NH_4^{+}, Ca^{2+}) play significant roles on the terrestrial and aquatic ecosystem via wet deposition; for instance, leading to severe soil (lake) acidification (alkalization), inhibiting the plant growth, and changing the regional climate (Liu et al., 2011; Yan et al., 2010; Larssen and Carmichael, 2000; Larssen et al., 1999). In the past decades,

China has been suffered from the severe air pollution along with the population growth and industrialization (Liu et al., 2016a). Therefore, the investigation of the wet deposition status of inorganic ions is of great interest to the public and policy makers (Négrel et al., 2007).

A large amount of studies mainly focused on the spatiotemporal variation of the S and N deposition around the world due to their adversely ecological effects in the past decades (Gerson et al., 2016; Clemens 2006; Zhang et al., 2010). Okuda et al. (2005) showed that the SO_4^{2-} concentration in the precipitation exhibited a slight decrease coupling with the decrease of the SO_2 concentration in Tokyo during 1990-2012. Hunová et al. (2014) reported that the averagely S deposition flux decreased from 181 kg/ha/year to 100 kg/ha/year in Czech during 1995 and 2011 on the basis of the data in 15 cities. Du et al. (2012) estimated that the wet deposition flux of inorganic nitrogen reached 3.5 kg N/ha/year according to the average of 151 monitoring in the United States during 1985-2012, which were significantly lower than that of China during the same period (11.11-13.87 kg/ha/yr) (Jia et al., 2014).

Many researches about the S and N deposition have been extensively performed to date in China in the recent years (Jia et al., 2014; Xu et al., 2015). In the past decades, the anthropogenic emissions of SO_2, NO_2, and NH_3 displayed the remarkable increase along with the dramatic increase of fossil fuel and fertilizer consumption in China (Jia et al., 2014; Kuribayashi et al., 2012). It was well documented that the gaseous precursors containing S and N could be transformed into sulfates (SO_4^{2-}), nitrates (NO_3^-), and ammonium (NH_4^+) during ageing in the atmosphere, thereby contributing to the formation of airborne fine particles, of which were considered to be the main reason for the persistent fog and haze pollution in China (Wang et al., 2016a; Qiao et al., 2015). At a city level, Huang et al. (2008) observed that the wet deposition fluxes of SO_4^{2-}, NH_4^+, and Ca^{2+}

displayed the slight decrease from 1986 to 2006 in the urban of Shenzhen, whereas the wet deposition of NO_3^- increased rapidly during the same period. Very recently, Pu et al. (2017) reported that the SO_4^{2-} concentration in the wet deposition of Shangdianzi (a regional background station of Beijing) showed slight decrease during 2003-2014, but the NO_3^- concentration showed an opposite trend. At a regional scale, Pan et al. (2013) observed that the highest S wet deposition was concentrated in the urban and industrial region of Tianjin among of ten sites of North China (NC). Song et al. (2017) suggested that the bulk deposition fluxes were in the order of Chengdu (urban) > Yanting (agricultural area) > Gongga mountain (natural reserve). At a national scale, Jia et al. (2014) firstly found that the wet deposition of N in Southeast China (SEC) showed a significant decrease, whereas it increased slightly in the western of China on the foundation of the data (620 monitoring sites) collected from 120 cities across China during 1990 and 2010. Following this work, Liu et al. (2016) further observed that the serious S deposition (79 monitoring sites) on SEC and Southwest China (SWC). In these studies, the spatial distributions of both S and N were determined using the spatial interpolation method, which generally required substantial monitoring sites (city > 150, and monitoring site > 300). However, these conclusions were obtained based on a small quantity of monitoring sites, which increased the uncertainties of the results. Meanwhile, the monitoring sites in these studies were mainly located on some remote regions such as mountain or rural site rather than the mixture of urban, suburban, and rural sites, which cannot accurately reflect the spatial variations of inorganic ions in China. Moreover, the spatiotemporal variations of other inorganic ions (i.e., K^+, Ca^+, Mg^{2+}) remained unclear to date, which were also linked to the acid deposition, as well as the haze pollution in China (Mikhailova et al., 2013; Aloisi et al., 2017; Müller et al., 2015).

Based on these field measurements, the ion levels in the deposition across China were believed to be underestimated due to the few ion species measured by previous studies (Liu et al., 2016a), which was closely associated with various emission sources (Kuang et al., 2016). Thus, the source identification should be performed to assess accurately their contributions to the wet deposition (Larssen et al., 1999). Liu et al. (2015b) identified that the Cl^- and NH_4^+ in the precipitation of Tibet were both originated from the marine and crustal source using the geochemical index method. On the basis of the positive matrix factorization (PMF) model, Qiao et al. (2015) showed that fossil fuel combustion and agriculture were the main sources of SO_4^{2-} and NO_3^- in Jiuzhaigou (Sichuan province). In a newly work reported by Leng et al. (2018), they supposed that the combustion of fossil fuels, domestic sewages, and fertilizers were the main sources of the N-bearing ions on the basis of the N isotope analysis. To date, some methods, including geochemical index method, multivariate analyses, and isotope signatures have been utilized to identify the anthropogenic versus natural sources of the inorganic ions in the precipitation. However, these methods suffered from some weaknesses from different standpoints (AlKhatib and Eisenhauer 2017; Shi et al., 2014). For instance, the geochemical index methods cannot estimate the contribution ratios of multiple sources to Ca^{2+} and Na^+ at a spatial scale (Liu et al., 2015b). Despite the advances of multivariate analyses lowering the associated uncertainties, the multi-collinearity still disturbed the predictions of these models (Shi et al., 2014). The isotope signature method was costly and complex, especially for the unconventional stable isotopes (i.e., K, Ca) (AlKhatib and Eisenhauer 2017), which restricted its application at a large scale. Therefore, multiple source apportionment methods should be combined in order to enhance the reliability of the results. Liu et al. (2015) also demonstrated that the geochemical index method coupled with multiple statistics decreased the uncertainties of results.

Apart from the source apportionment, the key factor identification for the ions in the wet deposition is also of great importance to reduce the acid deposition. At an early study, Singh and Agrawal (2008) revealed that the significant increase of vehicle emissions contributed to the accumulation of NO_2, which might be an important precursor of acid rain. Allen et al. (2015) observed that some inland cities in arid and semi-arid regions were generally subjected to dust events, which could increase the Ca^{2+} and K^+ concentrations in the wet deposition. Following this work, Yu et al. (2017a) found that considerable energy consumption, gross domestic production (GDP), and emitted substantial pollutants made China as major regions of acid rain around the world using path analysis and correlation analysis. However, these researches only assessed the limited factors for the inorganic ions in the wet deposition (Yu et al., 2016; Yu et al., 2017a), ignoring the contributions of other socioeconomic and natural factors. Moreover, these researches mainly focused the whole effects of the influential factors on inorganic ions at a national scale, while they did not consider the spatial heterogeneity of the influential factors, resulting possibly in the great deviation of the inorganic ions in the wet deposition for the different regions.

Here, the data of nine water-soluble ions in the precipitation including Ca^{2+}, Cl^-, F^-, K^+, Mg^{2+}, Na^+, NH_4^+, NO_3^-, and SO_4^{2-} in the 320 cities across the whole China were collected during 2011-2016 to examine the characteristics of the main water-soluble ions in the precipitation. Specifically, the objectives of our study were (1) to reveal the spatiotemporal patterns of water-soluble ions in the precipitation recently in China at a national scale; (2) to identify quantitatively the source of the water-soluble ions in the precipitation based on the multiple statistical methods; and (3) to seek out the key factors for the inorganic ions at a spatial scale. This study supplied the systematical data for comprehensive understanding on the inorganic composition in the precipitation based on the long-

term field measurement, at a national scale (the 1282 monitoring sites distributed in the 320 cities across the whole China), which was beneficial to the implementation of appropriate strategies to promote environmental protection in China.

2. Materials and methods

2.1 Site description

The spatial distribution of field stations in National Acid Deposition Monitoring Network (NADMN) is illustrated in Fig. 1. The selected 1282 monitoring sites are distributed in the 320 cities across 31 provinces. These cities are classified into Northeast China (NEC), NC, SEC, Northwest China (NWC), and Southwest China (SWC) (Tab. S1). Both of NEC and NC show typical temperature monsoon climate, while SEC presents the subtropical monsoon climate. The SWC region suffers from the combined effects of subtropical monsoon climate and tropical monsoon climate. NWC suffers from the temperate continental climate and displays minor rainfall amount. NEC and NC are filled with temperature deciduous forest, whereas SEC is mainly occupied by the subtropical evergreen forest. The subtropical evergreen forest and tropical evergreen forest spread out the SWC region. The NWC is generally filled with expansive grasslands and desert. The latitudes and longitudes of all of 1282 monitoring sites range from 18.25 to 50.78° *N*, and from 79.57 to 129.25° *E*, respectively. Annual mean rainfall ranges from 10 to 1853 mm and the annual mean air temperature varies between -6.9 and 24.3 °C. The monitoring sites were designed as a mixture of urban and background sites. 850 monitoring sites are concentrated in urban region, and 432 sites in suburban and rural areas are considered as the background sites.

2.2 Sampling and chemical analysis

The real-time precipitation was collected by monitors in the field stations as a routine procedure

of NADMN. Samples from each monitoring site were collected using wet deposition automatic collectors (diameter 30 cm) installed at 1.5 m above ground level. The cover of the collection instrument opened automatically without delay when the precipitation sensor was activated and closed automatically when precipitation ceased and no water remained on the sensor surface. The sample in each rain event was collected and these samples were collected in all of the monitoring sites simultaneously. Each sample was properly collected during the precipitation event when the wet-only deposition instrument was under the normal condition. After the sampling, the pH and EC values of the samples were measured immediately. The sample pH was measured using a pH meter (MP-6p, HACH, USA) at 20–25°C. The EC value of the precipitation samples was determined by an EC meter (CyberScan, CON1500, USA). After the analysis of pH and EC, all of the samples were contained in the pre-cleaned polyethylene plastic bottles at -18°C in order to prevent the possible transformation by microbes. All of the plastic buckets and the polyethylene plastic bottles were cleaned with deionized water for more than three times and then air-dried in clean room prior to use.

All of the precipitation samples were used to analyze the concentrations of the water-soluble ions including NO_3^-, Cl^-, Ca^{2+}, K^+, F^-, NH_4^+, Mg^{2+}, SO_4^{2-}, and Na^+. The microporous membranes (0.45 μm) were employed to remove all of insoluble particulates (< 0.45μm) from the precipitation samples before the analysis. The ion concentrations were determined through ion chromatography (Dionex ICS-900) equipped with a conductivity detector (ASRS-ULTRA). The CS12A column and AS11-HC column were applied to determine the cations and anions, respectively. Each sample was measured for more than three times and the relative standard deviation was less than 5% for each ion. Analysis of the blank samples once a month confirmed that the cross contamination in the

177 present research was negligible. For each ion, the analysis of simulated precipitation suggested that
178 the relative bias was lower than 10%.

179 2.3 Data calculation

180 The monthly and annual volume-weighted mean (VWM) concentrations were calculated based
181 on the concentrations of specific ions and precipitation. The monthly and annual VWM
182 concentrations were obtained as follows:

183 $$C_x = \frac{\sum_{i=1}^{n}(C_i(x) \times P_i)}{\sum_{i=1}^{n} P_i} \quad (1)$$

184 where C_x denoted the monthly and annual VWM concentration of the given ion; $C_i(x)$ was the
185 concentration of the given ion in the precipitation (μeq/L); P_i was the precipitation in individual
186 sample. The monthly and annual VWM pH values were obtained based on the corresponding VWM
187 concentrations of H^+ via Eq. (1).

188 The wet deposition flux of the given ion was calculated using the following Eq. (2)

189 $$D_w = P_t C_w / 100 \quad (2)$$

190 where D_w was the wet deposition flux of the given ion (kg N ha^{-1}); P_t was the total amount of the
191 precipitation events (mm); C_w was the VWM concentration of each ion (mg/L); and 100 was a unit
192 conversion factor.

193 In order to obtain the contributions of various alkaline species to acid neutralization in the
194 precipitation, the neutralization factor (NF) was calculated using the following Eq. (3)-(5)
195 (Kulshrestha et al., 1995):

196 $$NF_{NH_4^+} = \frac{NH_4^+}{NO_3^- + SO_4^{2-}} \quad (3)$$

$$NF_{Ca^{2+}} = \frac{Ca^{2+}}{NO_3^- + SO_4^{2-}} \quad (4)$$

$$NF_{Mg^{2+}} = \frac{Mg^{2+}}{NO_3^- + SO_4^{2-}} \quad (5)$$

2.4 Source apportionment of ionic species in wet deposition

The enrichment factor (EF) has been widely applied to estimate the contribution ratios of the various sources to the major ions in the previous studies (Lawson and Winchester 1979; Cao et al., 2009; Lu et al., 2011). In the present study, an ion EF in the precipitation relative to the ion in the sea was calculated using Na as a reference element as follows:

$$EF_{sea} = \frac{(X / Na^+)_{precipitation}}{(X / Na^+)_{sea}} \quad (6)$$

where EF_{sea} was the enrichment indicator of a given ion in the precipitation relative to the ion in the sea; X was the ion in the precipitation; $(X/Na^+)_{precipitation}$ represented the ratio of components in the precipitation; $(X/Na^+)_{sea}$ denoted the ratio of components in the sea (Keene et al., 1986; Turekian, 1968).

The EF value of an ion in the precipitation relative to the corresponding ion in the soil was calculated following Eq. (7):

$$EF_{soil} = \frac{(X / Ca^{2+})_{precipitation}}{(X / Ca^{2+})_{soil}} \quad (7)$$

where EF_{soil} represented the EF value of an ion in the precipitation relative to the corresponding ion in the soil; X denoted an ion in the precipitation; $(X/Ca^{2+})_{precipitation}$ was the ratio of components in the precipitation; $(X/Ca^{2+})_{sea}$ denoted the ratio of components in the soil (Wei et al., 1991; Wei et al., 1992; Shi et al., 1996; Zhang et al., 2012; Chen et al., 1992).

In order to quantify the anthropogenic source versus natural one of ionic species in the

precipitation. The fractions of anthropogenic, marine, and crustal source contributed to the ions in the precipitation were calculated as follows:

$$SSF = \frac{(X / Na^{+})_{sea}}{(X / Na^{+})_{precipitation}} \times 100\% \quad (8)$$

$$CF = \frac{(X / Ca^{2+})_{soil}}{(X / Ca^{2+})_{precipitation}} \times 100\% \quad (9)$$

$$AF = 100\% - SSF - CF \quad (10)$$

where *SSF* represented the fraction of sea salt; *CF* denoted the crustal contribution; and *AF* denoted the anthropogenic fraction. *SSF* was recalculated as the difference between 1 and *CF* when *SSF* was greater than 1; *CF* was recalculated as the difference between 1 and *SSF* when *CF* was higher than 1.

Factor analysis (FA) has been widely employed to determine the contribution ratios of natural and anthropogenic source to ionic species in the precipitation. First of all, FA was applied to reduce the dimension of original variables (measured ion concentrations in samples) and to extract a small number of principal components to analyze the relationships among the observed variables. All of the factors with eigenvalues over 1 were extracted based on the Kaiser-Meyer-Olkin (KMO) test and the Bartlett's test of sphericity, and were rotated using the Varimax method. The FA factor scores and each ion concentration were treated as independent and dependent variables, respectively. The resultant regression coefficients were employed to convert the absolute factor scores and then to calculate the contribution of each PC source (Luo et al., 2015).

2.5 The geographical weight regression (GWR) method

Although the relationships between the independent variables and the dependent variables could be calculated using correlation analysis and multiple linear regression analysis (MLR), these

methods cannot show the spatial variability of regression coefficients. Thus, the GWR method was applied to explore the effects of socioeconomic factors on wet deposition of inorganic ions in consideration of the spatial correlation. As an indicator to reflect the impacts of socioeconomic factors on inorganic ion depositions, local regression coefficients were obtained using weighted least squares with the following weighting function (Brunsdon et al., 1996):

$$\beta(u_i, v_i) = (X^{\mathrm{T}} W(u_i, v_i) X)^{-1} X^T W(u_i, v_i) Y \quad (11)$$

where $\beta(u_i, v_i)$ represented the local regression coefficient at city i; *X* was the matrix of the influential factors; *Y* denoted the matrix of the wet deposition fluxes of the water-soluble ions; and $W(u_i,v_i)$ was an n order matrix that the diagonal elements were the spatial weighting of the influential factors. The spatial weight function was calculated via the exponential distance decay form:

$$W(u_i, v_i) = \exp(-d^2(u_i, v_i) / b^2) \quad (12)$$

where $d(u_i,v_i)$ represented the distance between the location i and j, and b was the kernel bandwidth.

2.6 Data source and statistical analysis

The data of GDP, gross industrial production (GIP), N fertilizer use, vehicle ownership, urban green space (UGS) during 2011-2016 were collected from China City Statistical Book. Total energy consumption (TEC) during the period were obtained from China Energy Statistical Yearbook, which consisted of the consumption of coal, crude oil, and natural gas. The daily meteorological factors including precipitation, maximum and minimum air temperature, wind speed, air pressure, relative humidity (RH) during 2011-2016 were collected from China Meteorological Data Network. The daily visibility data during 2011-2016 was collected from National Centers for Environmental Prediction (NCEP). The data of dust days were calculated based on the horizon visibility data. The days with the visibility lower than 1 km were treated as the dust days. The daily data of $PM_{2.5}$, PM_{10},

SO_2, and NO_2 were downloaded from the National Environmental Monitoring Platform (https://www.aqistudy.cn/historydata/). These data at a national scale were open access since January 2014. To match the meteorological data at a national scale, the data of air pollutants during 2014-2016 were applied to investigate the relationships of the water-soluble ions, meteorological factors, and the air pollutants in the atmosphere (Tab. S2). In addition, the SR analysis was employed to determine the key factors regulating the wet deposition fluxes of the water-soluble ions. All of the statistical analysis were performed by the software package of ArcGIS 10.2, SPSS 21.0, and Origin 8.0 for Windows 10.

3 Results and discussion

3.1 The pH and EC values in the precipitation

To obtain the preliminary knowledge about the precipitation characteristics, the basic physiochemical properties including pH and EC of the precipitation samples are presented in Fig. 2. The annually pH during 2011 and 2016 ranged from 5.45 ± 0.27 (mean ± standard deviation) to 5.94 ± 0.46 and the mean value was 5.76 (Fig. 2a). Seinfeld (1986) estimated that the precipitation with pH lower than 5.60 was considered as acid rain because the pH value of natural water in equilibrium with atmospheric CO_2 was 5.60. However, the CO_2 level has been increasing in recent years and thus the equilibrium pH has changed (McGlade and Ekins 2015) Therefore, the average CO_2 concentration during 2011-2016 (396.83 ppm) around the world was applied to the present study (http://www.ipcc.ch/). The ionization equation of CO_2 include $CO_2+H_2O=H_2CO_3$ and $H_2CO_3=HCO_3^-+H^+$. The dissociation constant of two equations are 3.47×10^{-2} (K_0) and 4.4×10^{-7} (K_1), respectively. The $(c(H+))^2 = K_0\times K_1\times P_{CO2} = 6.06 \times 10^{-12}$. Therefore, the equilibrium pH was 5.61, which was slightly higher than the current value (pH = 5.60). Herein, 41% of the samples during

the measurement showed the pH value below 5.61. Compared with the pH value of the precipitation during 1980-2000 (Wang and Xu 2009), the pH value of the precipitation showed a remarkable increase in recent years. For instance, the pH value in the precipitation of SWC increased from 3.5-4.0 (the mean value of 1980-2000) to 5.87 during 2011-2016. Although some cities in Hunan and Hubei province (e.g., Chengzhou, Erzhou) still suffered from the severe acid deposition, the mean pH values (4.46) of the two provinces during 2011-2016 were slightly higher than those in 1980-2000 (3.5-4.0). It was well known that precipitation pH was associated with the SO_2 and NO_x emissions (Pu et al., 2017). Due to the implementation of SO_2 control measurements since the 11th Five-year Plan, the SO_2 column concentration over China displayed a marked decrease after 2007 based on Global Ozone Monitoring Experiment (GOME), reported by Gottwald and Bovensmann (2011). Based on the bottom-up method, Liu et al. (2010) also supposed that SO_2 emission began to decrease since 2007, in good agreement with the results obtained from the remote sensing. Besides, nearly all of the power plants built newly and the in-use plants have been required to be equipped with advanced selective catalytic reduction (SCR) or selective non-catalytic reduction (SNCR) since 2010 (Tian et al., 2013; Lu et al., 2011), resulting in a gradual decrease of the NO_x emission after 2010 (China Statistical Yearbook, http://data.stats.gov.cn/easyquery.htm?cn=C01). Based on the result of correlation analysis (Tab. S2), the pH value showed the significantly negative correlation with SO_2 and NO_2 in the ambient air especially with the increased RH. Thus, it could be proposed that the pH value of the precipitation in most of the regions of China during 2011 and 2016 were significantly higher than those before 2000 because the SO_2 and NO_x emissions during 2011-2016 were lower than those before 2000.

The pH value in the precipitation at a national scale exhibited significantly seasonal variation

with the highest value in summer (6.57), followed by autumn (5.64), spring (5.49), and the lowest one in winter (5.32) (Fig. 2b). The seasonal variation of pH values in wet deposition was supposed to be linked with the wash-out effect of precipitation on atmospheric particular matters (Xing et al., 2017), which was supported by the positive relevance between pH and precipitation ($p < 0.01$). Besides, the scavenging atmospheric SO_2 by precipitation may also play an important role in the seasonal variation of the pH values (Wu and Han, 2015). The atmospheric SO_2 concentration was the lowest in summer and the highest in winter. The highest atmospheric SO_2 and sulfate concentrations in winter of the north part of China were partially ascribed to the intensive domestic coal combustion for heating (Liu et al., 2016b; Liu et al., 2017).

At a spatial scale across the whole China (Fig. 3a), the pH value of the precipitation presented a gradual increase from SEC to NC and NWC. The relatively low pH values in the precipitation were usually observed in YRD (i.e., Huzhou, Ningbo, and Shanghai), Hunan province (i.e., Changde, Changsha, and Loudi), Hubei province (i.e., Wuhan), and Jiangxi province (i.e., Nanchang, Yichun, and Jingdezhen), but the relatively high pH values occurred in NC and NWC, especially in Xinjiang autonomous region (i.e., Changji, Altai, Urumqi and Aksu). Among of the 320 cities, the lowest one and the highest one were located in Huzhou, (3.20, Zhejiang province), and Altai, (6.82, Xinjiang autonomous region), respectively (Fig. 3). Compared with high acidity in some cities of SEC, the acidity of the precipitation in many cities of NC could be largely neutralized by some alkaline ions because the saline-alkali soils were widely distributed in NC (Wang et al., 2014). Some city atmosphere (i.e., Urumqi and Altay) in Xinjiang autonomous region were frequently attacked by local continental dust particles, diluting the precipitation acidity (Rao et al., 2015).

The annually mean EC varied from 10.18 ± 3.21 μS cm^{-1} to 13.33 ± 3.75 μS cm^{-1} during the

period (Fig. 2a). The EC value was mainly affected by total water-soluble ions in the precipitation and rainfall amount, of which indirectly reflected the cleanliness of the precipitation and the air pollution status. The decrease of EC in recent years suggested that air pollution in China has been mitigated due to the implementation of special air pollution control measures (Wang et al., 2017; Yang et al., 2016). The EC value also presented distinctly seasonal variation and showed the highest value in spring (Fig. 2c), followed by ones in summer and autumn, and the lowest one in winter, which was apparently different from the seasonal pH variation. Among all of the inorganic ions, only Ca^{2+} displayed notable relationship with EC ($p < 0.01$). It was supposed that many crustal ions such as Ca^{2+} could be lifted up and transported to East China by frequent dust storms in spring and summer, thereby leading to the high EC value in the precipitation (Fu et al., 2014). The mean EC value exhibited a significantly spatial variation with the higher ones in Shizuishan (36.60 $\mu S\ cm^{-1}$) and Yinchuan (24.79 $\mu S\ cm^{-1}$) (Ningxia autonomous region), Wuwei (60.01 $\mu S\ cm^{-1}$) (Gansu province), Edors (28.72 $\mu S\ cm^{-1}$) (Inner Mongolia autonomous region), and Aksu (22.06 $\mu S\ cm^{-1}$) (Xinjiang autonomous region) and the lower one in some remote regions such as Lhasa (3.42$\mu S\ cm^{-1}$) (Tibet autonomous region), Aba (2.20 $\mu S\ cm^{-1}$) (Sichuan province) and Diqing (2.46) (Yunan province) (Fig. 3b). The lowest and highest EC were observed in Aba (2.20 $\mu S\ cm^{-1}$) and Wuwei (60.01 $\mu S\ cm^{-1}$), respectively (Fig. 3). The cities in the western and northern of Sichuan province, and the southern of Tibet autonomous region presented the lower EC values due to the sparse population and minimal industrial activity. Although TB has received the effects of the industrial emissions and biomass burning from South Asia via a long-range atmospheric transport, most of the pollutants tended to be deposited on the South of Himalayas except persistent organic pollutants (POPs) (Yang et al., 2016b; Dong et al., 2017). The cities with higher EC was generally close to the

Taklamakan and Gobi deserts. Strong winds in these deserts stirred a large amount of dusts, and then caused many dust events, resulting in high loading of Ca^{2+} and Mg^{2+} (Wang et al., 2016d). The positive relationship between wind speed and EC also revealed that strong wind promoted the accumulation of crustal ions over China (Tab. S2).

3.2 Chemical composition in the precipitation

3.2.1 The inter-annual variation of the water-soluble ions

The inter-annual variation of the ionic constitutes of the precipitation in China during 2011-2016 are summarized in Fig. 4. The concentrations of Na^+, NO_3^-, and SO_4^{2-} increased from 7.26 ± 2.51, 11.56 ± 3.71, and 33.73 ± 7.59 μeq/L to 11.04 ± 4.64, 13.59 ± 2.63, and 41.95 ± 8.64 μeq/L during 2011 and 2014, respectively (Fig. 4a). However, Na^+, NO_3^-, and SO_4^{2-} concentrations decreased from the highest ones in 2014 to 9.75 ± 2.89, 12.29 ± 4.02, and 30.57 ± 7.43 μeq/L in 2016. The concentrations of Ca^{2+}, NH_4^+, and Mg^{2+} increased from 31.59 ± 8.29, 14.84 ± 4.63, and 8.77 ± 2.42, to 58.84 ± 10.31, 41.33 ± 10.26, and 10.49 ± 3.07 during 2011-2013 (Fig. 4a), whereas they decreased from the peak values in 2013 to 31.20 ± 8.48, 18.13 ± 4.84, and 8.93 ± 2.92 μeq/L in 2016, respectively. The F^- concentration exhibited gradual decrease from 3.63 to 2.96 μeq/L during 2012-2016. However, the K^+ and Cl^- concentration fluctuated during 2011 and 2016 and did not display regularly annual variation.

It was well documented that the SO_4^{2-} concentration was closely associated with the SO_2 emissions because SO_2 in the ambient air could be transformed into SO_4^{2-} during aging in the atmosphere (Qiao et al., 2015). In the present study, SO_4^{2-} in the precipitation exhibited a marked correlation with SO_2 in the ambient air ($p < 0.01$), especially with the increased RH (Tab. S2). The total SO_2 emissions in China decreased dramatically due to the installation of the flue gas

desulfurization (FGD) systems and the closure of less efficient power plants in China since 2012 (Li et al., 2017b). At a national scale, the remarkable decrease of the SO_4^{2-} concentration was observed since 2014, which lagged behind the decrease of the SO_2 emission. Such scenario was widely observed in some developed countries such as Japan (Okuda et al., 2005). However, some cities (i.e., Beijing and Baoding) in NC showed the notable decreases since 2012, which corresponded to the decrease of the total SO_2 emission. It was supposed that the electrostatic precipitators (ESP) and fabric filters (FFs) for the sulfates removal were more widely applied to steel and iron plants, and cement production process, both of which were widely distributed in NC (Hua et al., 2016; Wang et al., 2016b). Moreover, coal has been gradually replaced by natural gas for domestic heating in Beijing, resulting in the less SO_2 emission and thus decreasing the SO_2 concentration in the ambient air (Pu et al., 2017). Based on the open data downloaded from National Environmental Monitoring Platform, the annually mean SO_2 concentration in Beijing decreased from 22.0 $\mu g/m^3$ to 9.29 $\mu g/m^3$ during 2014-2016, in good agreement with the temporal variation of SO_4^{2-} in the precipitation.

The NO_x emission decreased rapidly after the upgrading of oil product quality standards, the import denitrification facilities, and the implementation of low-NO_2 burner technologies (Li et al., 2016; Liu et al., 2017). However, the NO_3^- concentration in the precipitation over China only displayed slight decrease during this period, which was in good agreement with the slight decrease of national NO_2 concentration in the atmosphere (Zhan et al., 2018). It suggested that stricter controls on NO_x emissions from power plants might be counteracted by the increase of power plants and energy consumption (Liu et al. 2015a; Wang et al. 2018). Besides, it was assumed that the high NO_3^- in the precipitation resulted from the increase of motor vehicles (Link et al., 2017). Based on

392 the bottom-up method, the estimated NO_x emissions from vehicle exhausts in China linearly
393 increased by 75% since 1998 (Wu et al., 2016). Shandong suffered from the highest vehicle
394 emissions among all of the provinces, of which the NO_x released from vehicle exhausts in Shandong
395 province increased from 477.6 Gg to 513.8 Gg during 2011-2014 (Sun et al., 2016), corresponding
396 to the annual variation of NO_3^- in the precipitation of Jinan and Linyi. The NO_3^-/SO_4^{2-} value was
397 recognized as an important index to determine the relative importance of nitrate (mobile) vs. sulfate
398 (stationary) emission in the atmosphere (Arimoto et al., 1996). The value of NO_3^-/SO_4^{2-} at the
399 national scale was still lower than 1, suggesting that the contribution of sulfate to the acidity of the
400 precipitation was still higher than that of NO_3^-. Nevertheless, the ratio in the precipitation showed a
401 gradual increase from 0.33 to 0.40 during this period, indicating that the precipitation type in China
402 has evolved from sulfuric acid type to a mixed type controlled by sulfuric and nitric acid.
403 The NH_4^+ level in the precipitation was closely linked to the NH_3 emission because NH_3 tended
404 to be neutralized to form $(NH_4)_2SO_4$ and NH_4NO_3 in the atmosphere (Zhang et al., 2016). The
405 anthropogenic emission of NH_3 was mainly derived from fertilizer use, livestock manures, vehicle
406 exhausts, and industrial processes (Kang et al., 2016). Wherein, livestock manures and synthetic
407 fertilizer application were considered as two major source of the NH_3 emission, accounting for 80-
408 90% of total emission (Kang et al., 2016; Xu et al., 2016). The nitrogen fertilizer consumption has
409 decreased since 2013 (http://www.stats.gov.cn/), which was in good agreement with the variation of
410 the NH_4^+ concentration in the precipitation. Therefore, the fertilizer consumption could be treated
411 as an important factor for the NH_4^+ level in the precipitation. However, the NH_3 emission from
412 livestock manures estimated by Kang et al. (2016) showed an opposite variation to the NH_4^+ level
413 in the precipitation collected herein. It was probably attributed to the slight decrease of air

414 temperature in the major cities of China during 2011-2013 because the actual NH_3 emission to the
415 atmosphere was sensitive to air temperature (Kang et al., 2016), which has been proved by the
416 correlation analysis (Tab. S2). Apart from the contribution source mentioned above, soil served as
417 major natural sources of the NH_3 emissions (Sun et al., 2014). Teng et al. (2017) demonstrated that
418 urban green space made a great contribution to the NH_3 amount in the atmosphere. In the present
419 study, the urban green space in some cities such as Lianyungang (Jiangsu province) and Qingdao
420 (Shandong province) showed the marked correlation with the NH_4^+ level in the wet deposition.
421 The long-range transport of dust aerosol was considered as the major source of Ca^{2+} and Mg^{2+}
422 in the atmosphere (Fu et al., 2014). Song et al. (2016) reported that the magnitude of dust emissions
423 in spring generally decreased in the past decades. The dust deposition and ambient PM_{10}
424 concentration in the Xinjiang autonomous region also decreased dramatically during 2000-2013
425 (Zhang et al., 2017a). Here, Ca^{2+} and Mg^{2+} in the wet deposition of some cities such as Aksu in
426 Xinjiang autonomous region decreased from 32.37 to 4.80 μeq/L and from 15.80 to 4.81 μeq/L
427 during 2011-2016, respectively, corresponding to the decrease of dust deposition. However, the
428 decrease of Ca^{2+} and Mg^{2+} over China significantly lagged behind the reduction of dust deposition.
429 It was well known that the increase of soil particles and dusts due to urbanization might induce the
430 high level of Ca^{2+} and Mg^{2+} in the wet deposition (Lyu et al., 2016). The road mileage in China
431 increased by 25% from 2011 to 2013, while it only showed slight increase (2.52%) during 2013-
432 2016 (http://www.stats.gov.cn/). Padoan et al. (2017) also demonstrated that the resuspension of
433 road dust generally showed the highest impact on the emission of the Ca and Mg elements among
434 non-exhaust sources (i.e. tire wear, brake wear, road dust).
435 Both of K^+ and Cl^- were identified as the important tracers for biomass burning and fireworks

436 (Cheng et al., 2014). Nevertheless, the K^+ and Cl^- concentration in the precipitation did not reflect
437 the contribution of biomass burning because biomass burning usually occurred in dry seasons (Zhou
438 et al., 2017b). Furthermore, the K^+ concentration in the precipitation showed significantly
439 relationship with crustal ions (Ca^{2+} ($r = 0.40$, $p < 0.01$) and Mg^{2+} ($r = 0.49$, $p < 0.01$)) (Tab. S2),
440 suggesting that other sources could play important role on the accumulation of K^+ and Cl^-. Chen et
441 al. (2017b) recommended that fugitive dust to be the main source of K^+ when the mitigation
442 measures were seriously implemented. The minor F^- in the wet deposition served as an indicator of
443 coal combustion because fluorine was generally released from coal combustion (Chen et al., 2013).
444 Recently, the F^- emission displayed remarkable decrease because more coal-fired power plants were
445 equipped with FGD and dust removal equipment (Zhao and Luo, 2017), which explained the
446 decrease of F^- in the precipitation of some industrial cities such as Baoding (3.22 to 1.65 during
447 2012-2016), Shijiazhuang (3.18 to 2.73), and Handan (3.88 to 3.53) in Hebei province. Na^+ was
448 generally originated from the transport of sea salt aerosols, fugitive dusts, and the incineration of
449 wastes and fossil fuels (Zhao et al., 2011). The Cl^-/Na^+ value in the precipitation of some coastal
450 cities (i.e. Lishui (1.15), Jiaxing (1.20), Dandong (1.18), Wenzhou (1.18)) were similar to the marine
451 equivalent Cl^-/Na^+ ratio (1.17) (Wang et al., 2015a), suggesting that Na^+ in the precipitation of these
452 coastal cities might be derived from ocean. However, the Cl^-/Na^+ ratios in the precipitation of some
453 regions far from the ocean were significantly higher than marine equivalent Cl^-/Na^+ ratio due to the
454 contribution of coal combustion (Liu et al., 2016b; Liu et al., 2017).
455 3.2.2 The seasonal variation of the inorganic ions in the wet deposition
456 Overall, the mean concentrations of SO_4^{2-}, NO_3^- and F^- in the wet deposition were in the order
457 of winter (SO_4^{2-}, NO_3^- and F^-: 45.74, 19.44 and 6.10 μeq/L) > spring (42.61, 13.83, and 3.45 μeq/L) >

458 autumn (28.85, 9.73, and 2.67 μeq/L) > summer (19.26, 7.66, and 2.04 μeq/L) (Fig. 4b). However,
459 the seasonal variation of inorganic ions still showed the slight difference between North China and
460 South China. The mean concentrations of SO_4^{2-}, NO_3^- and F^- in the precipitation of North China
461 displayed the highest in winter (47.88, 13.79, and 5.24 μeq/L), followed by those in spring (47.02,
462 10.18, and 3.64 μeq/L), autumn (32.20, 10.08, and 2.73 μeq/L), and summer (22.75, 6.29, and 1.69
463 μeq/L). However, NO_3^- in South China showed the highest level in spring (27.66 μeq/L). It was well
464 known that SO_4^{2-} and NO_3^- were usually generated via the oxidation of SO_2 and NO_2 in the
465 atmosphere, respectively (Yang et al., 2016). The combustion of fossil fuels for domestic heating in
466 winter probably promoted the accumulations of SO_2 and NO_2 in the atmosphere (Liu et al., 2017;
467 Lu et al., 2010). The cities in North China showed the higher SO_4^{2-} and NO_3^- levels in the
468 precipitation of winter compared with those in summer, which were in agreement with the seasonal
469 variations of SO_2 and NO_2 concentrations in the ambient air. It reflected that the combustion of
470 fossil fuels for domestic heating contributed to the accumulation of SO_4^{2-} and NO_3^- and these ions
471 deposited via the rainfall. Nevertheless, the acidic ions in the cities of South China were not always
472 in agreement with those in North because coal combustion for heating in winter was not widespread.
473 The NO_3^- level in South China showed the highest one in spring due to the effects of meteorological
474 factors. The stagnant meteorological conditions including shallow mixing layers, high atmospheric
475 pressure, low precipitation, and low wind speed occurred frequently in winter, thereby trapping
476 more pollutants and elevating the concentrations of SO_2 and NO_2 in the atmosphere (Tai et al., 2010).
477 In contrast, strong solar radiation and turbulent eddies from ocean in summer could promote the
478 dispersion of these pollutants (Antony Chen et al., 2001). For instance, some coastal cities such as
479 Beihai (Guangxi autonomous region) and Haikou (Hainan province) were generally exposed of

480 strong solar radiation and high wind speed, which significantly decreased the SO_4^{2-} and NO_3^-
481 concentrations in the precipitation of summer (Beihai: SO_4^{2-} (6.06) and NO_3^- (7.37); Haikou: SO_4^{2-}
482 (5.33) and NO_3^- (4.96)), whereas they usually displayed the higher value in spring due to the scarce
483 rainfall amount. The F^- concentration in the precipitation displayed the similarly seasonal variation
484 to SO_4^{2-} and NO_3^-, which was likely associated with the higher coal consumption for domestic
485 heating in some industrial cities of NC, NWC, and NEC (Ding et al., 2017).

486 The concentrations of Cl^-, Ca^{2+}, K^+, NH_4^+, Mg^{2+}, and Na^+ exhibited the highest values in summer,
487 followed by those in spring and autumn, and the lowest one in winter. The higher concentration of
488 NH_4^+ in the precipitation collected in summer was probably linked to agricultural activities. The
489 widespread utilization of fertilizer in summer have been observed over China (Zhang et al., 2011;
490 Tao et al., 2016), which could increase the NH_3 emission. In addition, the NH_3 emission was
491 sensitive to the air temperature and generally increased with the temperature (Kang et al., 2016).
492 The NH_3 released from agricultural activities could transform to NH_4^+, especially under the
493 condition of high RH (Li et al., 2013). Thus, the high NH_3 emission and rapid photochemical
494 reaction contribute to the higher NH_4^+ in the precipitation in summer. However, K^+, Ca^{2+}, and Mg^{2+}
495 displayed higher concentrations in spring and summer, which was probably related to the high
496 loading of fugitive dusts (Zhang et al., 2017c). Lyu et al. (2016) demonstrated that the high
497 temperature coupled with strong wind caused the lower water content in the road, leading to higher
498 tendency of dust re-suspension in the Wuhan summer. In the present study, these crustal ions in the
499 precipitation also showed the higher values in the summer of Wuhan. The high concentration of Na^+
500 and Cl^- in spring and summer was probably attributed to the evaporation of sea salt under the
501 condition of high air temperature (Grythe et al., 2014). It was found that Na^+ in summer were 5.1-

10.3 times of those in winter in some coastal cities such as Qingdao (5.96) (Shandong province), Qinhuangdao (9.65) (Hebei province), and Sanya (6.83) (Hainan province).

3.2.3 Spatial distribution of the water-soluble ions across the whole China

At a spatial scale, the annual mean concentrations of NO_3^-, Cl^-, Ca^{2+}, K^+, F^-, NH_4^+, Mg^{2+}, SO_4^{2-}, and Na^+ ranged from 0.20 to 47.98 μeq/L, from 0.27 to 80.86 μeq/L, from 0.59 to 157.15 μeq/L, from 0.15 to 23.43 μeq/L, from 0.11 to 11.64 μeq/L, from 0.20 to 84.24 μeq/L, from 0.28 to 39.30 μeq/L, from 0.29 to 191.95 μeq/L, and from 0.15 to 39.50 μeq/L during 2011-2016, respectively. All of these water-soluble ions displayed significantly spatial variation, as shown in Fig. 5 and Fig. 6.

The mean concentrations of the secondary ions (NO_3^-, NH_4^+, and SO_4^{2-}) showed the highest values in YRD (Changzhou (34.53, 73.40, and 80.47 μeq/L) (Fig. 5a-c) and Nanjing (35.62, 17.12, and 49.51 μeq/L) and SB (Chengdu (38.08, 65.19, and 57.16 μeq/L) and Leshan (25.32, 38.99, and 61.24 μeq/L)), followed by ones in NC (Jinan (11.67, 16.57, and 58.28 μeq/L) and Anyang (20.46, 41.32, and 22.01 μeq/L), and the lowest ones in TB (0.50, 0.91, and 1.44 μeq/L) (Lhasa). Many secondary ions exhibited the high concentrations in YRD because of intensive energy consumption and industrial activities (Zhou et al., 2017a). For instance, the total energy consumption of the Jiangsu province was second to Hebei province among all of the provinces in China (Wang 2014). The SO_2 and NO_x emissions from cement plants and iron and steel industries in Jiangsu and Zhejiang province were significantly higher than those in other provinces (Hua et al., 2016; Wang et al., 2016b), which was in coincident to the spatial agglomeration of the SO_2 and NO_2 concentrations in the ambient air of these provinces It has been reported that the acid deposition pattern have moved from SWC to SEC since 2000s (Yu et al., 2017a). However, SB still possessed high concentrations

of secondary ions in the precipitation because of high S content in the local consumed coals (Ren et al., 2006). Besides, the unique topographic conditions and unfavorable diffusion conditions facilitated the deposition of regionally transported pollutants stuck by Qinling mountains and Daba mountain (Kuang et al., 2016), although the energy consumption of Sichuan province was much less than those in other provinces (Tian et al., 2013). Moreover, the steady increase use of fertilizer and livestock manures coupled with high air temperature made SB to be one of the NH_3 emission hotspots (Li et al., 2017a). Nevertheless, some remote areas in NWC and SWC such as Lhasa and Aba showed the lower secondary ions due to sparse population and anthropogenic activities (Li et al., 2007). In these regions, these secondary ions were mainly derived from crustal source, and then deposited concurrently in the rainfall events (Niu et al., 2014). Besides, relatively extensive anthropogenic activities such as increased vehicle exhaust might promote the emissions of secondary ions in the tourist season (Qiao et al., 2017). For instance, the number of tourists in Lhasa have been increasing to 11 million until 2015 (http://www.xinhuanet.com/fortune/2016-01/13/c_1117763885.htm), which could boost the slight increase of secondary ions in the wet deposition.

F^- showed the higher concentrations in NC, YRD, and SB because many coal-fired power plants and iron and steel industries were mainly concentrated in the Hebei and Jiangsu province (Liu et al., 2015a) (Fig. 6a). Besides, Hebei and Jiangsu were two provinces with much higher coal consumptions (Li et al., 2017), which could release large quantity of F^- to the atmosphere. Although the power plants and iron and steel industries were relatively scarce in SB, many large phosphorite mines might increase the F^- concentration in the precipitation (Wu et al., 2014). As one of the largest phosphorite mine over China, Jinhe phosphorite mine was close to Chengdu, which significantly

increased the F^- concentration in the precipitation of Chengdu (9.21 μeq/L). Moreover, the high abundance of F^- in the local coal (Mianyang: 269.25 μg/g, Guangan: 1061μg/g) also contributed to the F^- emissions (Dai and Ren, 2006; Wang et al., 2016c; Ren et al., 2006). In addition, the F^- in the precipitation showed remarkable relevance with T_{max} based on the correlation analysis ($r = 0.12$, $p < 0.05$). The annually mean air temperature in SB (17.2 ℃) were slightly higher than that in Hebei (14.3 ℃) and Jiangsu (16.4 ℃) province, thereby boosting the F^- emission.

The high concentrations of Cl^- were mainly concentrated on coastal cities such as Shanghai, Lianyungang (Jiangsu province) and Qingdao (Shandong province) (Fig. 6b), indicating the effect of sea-salt sourced from the ocean (Gu et al., 2011; Allen et al., 2015; Grythe et al., 2014). The high Na^+ concentration not only focused on these coastal cities (Fig. 6c), but also enrich in some arid and semi-arid cities such as Jinchang (35.08 μeq/L) and Gannan (25.51 μeq/L) (Gansu province). It was assumed that the windblown dust originated from Taklimakan Desert could play a vital role on the enrichment of Na^+ in Inner Mongolia and Hexi corridor because these regions were located on the downwind direction of dust (Engelbrecht et al., 2016). Meanwhile, the evaporation of salt lakes in West China might promote the Na^+ enrichment in the precipitation (Bian et al., 2017). Besides, the dust event also promoted the elevation of Ca^{2+}, especially in Jiayuguan and Guyuan (Gansu province) (Fig. 6d), both of which were located in the Hexi corridor (Allen et al., 2015). The Mg^{2+} presented higher value in some cities (Handan: 36.63 μeq/L, Liupanshui: 39.30 μeq/L) in the Hebei province and Guizhou province (Fig. 6e). The soil in the Guizhou province possessed the highest Mg concentration (843.33 mg/kg) in China (Li et al., 1992), where the Mg^{2+} stored into the soils could be lifted into the atmosphere by strong wind coupled with severe stony desertification (Jiang et al., 2014). Although the Mg concentration in the soil of Hebei province was slightly lower compared

with those of Guizhou province, the bioavailable Mg concentration peaked in Hebei province (Hao et al., 2016), which could be inclined to re-suspend into the atmosphere and then deposit with the rainfall in the warm season.

3.2.4 Neutralization capacity of the alkaline ions

In order to reveal the most important ion for neutralization (Ca^{2+}, NH_4^+, and Mg^{2+}) in the precipitation, the relative proportion of three NFs in all of the cities are summarized in Fig. 7. The triangular diagram showed that the contribution of three ions were in the order of Ca^{2+} (51.84%) > NH_4^+ (34.14%) > Mg^{2+} (14.02%). The NF ratios of NH_4^+ and Ca^{2+} in China displayed the highest values in summer, followed by ones in spring and autumn, and the lowest one in winter (Fig. 7a). It was supposed that strong acid neutralization were mainly brought about by the alkaline ions via high rainfall. Besides, the neutralization capacity of the alkaline ions reached higher in spring due to the effects of dust events (Wang et al., 2015b). In the present study, the NFs of NH_4^+ and Ca^{2+} in Beijing (NH_4^+: 0.57, Ca^{2+}: 0.17) and Baoding (NH_4^+: 0.56, Ca^{2+}: 0.19) showed the markedly higher values in spring. Zhai and Li (2003) also observed that most frequent dust storms generally occurred in NC in spring. However, the NFs of Mg^{2+} (0.70) showed the highest one in winter. Aside from the temporal difference of neutralization, the NFs presented a significantly spatial variation in China (Fig. 7b). The high NFs of Ca^{2+} were mainly concentrated on some cities in NWC such as Bayingolin (0.57) because these arid and semi-arid regions were exposed of periodic Asian dust intrusions (Yu et al., 2017b). In the case of the typical dust events, the content of crustal species such as Ca increased substantially (Chen et al., 2015). Compared with the other regions, the NFs of NH_4^+ showed the higher value in some cities of SWC such as Chengdu (0.55). Kang et al. (2016) demonstrated that the NH_3 emissions in Sichuan province were significantly higher than those in

other provinces of China, accounting for more than 10 % of the total emission from livestock manures. The NFs of Mg^{2+} peaked in NC, which was in good agreement with the higher concentration of Mg^{2+} in the wet deposition of NC. The higher concentration of bioavailable Mg^{2+} in the soil was beneficial to increase the neutralization capacity of Mg^{2+} in the wet deposition (Hao et al., 2016), although the SO_2 and NO_2 emissions in NC were significantly higher than those in other regions (Fu et al., 2016).

3.3 Comparisons of pH, EC, and the inorganic ion concentrations with the previous studies

The annual mean pH, EC and the inorganic ion levels in the precipitation of some metropolitans across China are summarized in Tab. 1. The mean pH values of the most cities in SEC and SWC (i.e., Shanghai: 4.39 and Wuhan: 4.68) were lower than those in some remote areas such as Jiuzhaigou (5.95) and Yulong mountain (5.94) (Qiao et al., 2018; Niu et al., 2014), while the average pH values of some cities in NC and NWC such as Zhengzhou (6.09) and Urumqi (6.13) were slightly higher than those in remote areas. It was assumed that the remote areas were less affected anthropogenic source except local tourist activities, while high aerosol emissions were mainly centered on some metropolitans of SEC and SWC. The pH of the precipitation in Zhengzhou (pH = 6.09) (Henan province) and Urumqi (pH = 6.13) (Xinjiang autonomous region) showed high value compared with some remote regions because of the strong neutralization capacity of alkaline ions (Wang et al., 2014). Besides, the pH values in the wet deposition of most metropolitans in China were also lower than those in some developing countries (e.g., Guaiba: 5.92, Petra: 6.80) (Tab. 1). It was supposed that SO_2 and NO_x emitted from industrial and vehicle emissions in China could be higher than those in some countries such as Brazil and Jordan (Wu and Han 2015). In addition, higher abundance of the neutralizing components in Jordan tended to increase pH of the

precipitation. On the other hand, the pH values of the wet deposition in most cities of China were significantly higher than those in some cities of developed countries such as Sardinia (pH = 5.18) (Italy) and Adirondack (pH = 4.50) (United States). It was assumed that many Western countries were faced up with severe acid issue due to the rapid industrialization before 2002 (Sickles II and Shadwick 2015). In addition, the annually mean rainfall amount in some cities of East China were higher than those in Sardinia and Adirondack, which could dilute the acidity of the precipitation (Tsai et al., 2011). The mean EC in the wet deposition of most cities over China were approximate to those in some remote regions (i.e., Yulong Mountain, Jiuzhaigou), and some foreign cities such as Guaiba, Brazil. However, Lanzhou (EC = 58.06 μS cm^{-1}) (Gansu province) and Petra (EC = 160 μS cm^{-1}) (Jordan) showed remarkably higher value than other cities, suggesting that the dust cyclones from Taklamakan and Khamaseen played vital roles on the EC and chemical composition in the precipitation (Abed et al., 2009).

The concentrations of NO_3^-, SO_4^{2-}, and NH_4^+ in the most cities of China except Qingdao (Shandong province) and Lhasa (Tibet autonomous region) were significantly higher than those in some natural reserve areas such as Jiuzhaigou, Yulong Mountain, and Nam Co (Qiao et al., 2018; Niu et al., 2014) (Tab. 1), suggesting the local point and non-point emissions in these cities played important roles on the concentrations of inorganic ions in the precipitation. However, the concentrations of these inorganic ions in the most cities were lower than those in foreign cities such as Singapore, Petra (Jordan), Tokyo, and Newark (United States) (Balasubramanian et al., 2001; Al-Khashman et al., 2005; Okuda et al., 2005; Song and Gao 2009), indicating the effects of restricting emissions of air pollutants since Chinese 12th Five-Year Plan (Liu et al., 2016a). However, some cities including Shenyang (Liaoning province) and Chengdu (Sichuan province) were still faced up

with severe acid deposition. On the whole, the concentrations of the crustal ions (Ca^{2+} and Mg^{2+}) were in the order of the arid and semi-arid cities/regions (Nam Co, Urumqi, Lanzhou, and Petra) > the inland cities and natural reserve regions (Chengdu and Yulong mountain) > the coastal cities (i.e., Guaiba, Singapore, and Tokyo). Kang et al. (2016) reported that Tibetan Plateau have been frequently affected by dust events under the condition of climate change in the past decades, which probably increased the Ca^{2+} and Mg^{2+} levels in Nam Co. However, it should be noted that some coastal cities such as Patras (Greece) and Sardinia (Italy) possessed higher Ca^{2+} and Mg^{2+} levels, which was probably attributed to the long transport of the dust from of the Sahara desert (Kabatas et al. 2014). Cabello et al. (2016) demonstrated that African air masses mostly reached some coastal cities of Mediterranean on the basis of back-trajectory analysis.

3.4 The source apportionment of the ions in the precipitation across China

3.4.1 EF and geochemical index method

The mean values of EFs (seawater and soil), SSF and CF in all of the cities are listed in Tab. 2. The water-soluble ion was treated to be enriched relative to the reference source when the EF value of the ion was significantly higher than 1.00, whereas it was considered to be diluted when the EF value of the ion was not much higher than 1.00. In the present study, the mean EF_{sea} for Na^+, Cl^-, SO_4^{2-}, NH_4^+, K^+, Mg^{2+}, Ca^{2+}, NO_3^-, and F^- over China were 1.00, 1.13, 7.22, 10.51, 16.16, 18.18, 231.56, 3507.49, and 5864.28, suggesting that Cl^- and Na^+ in the precipitation were enriched in the marine origin at a national scale. The mean EF_{soil} of Mg^{2+}, K^+, Ca^{2+}, Na^+, SO_4^{2-}, F^-, NO_3^-, NH_4^+, and Cl^- reached 0.55, 0.83, 1.00, 1.83, 5.13, 9.96, 59.36, 86.31, and 169.88, indicating that Ca^{2+}, K^+, and Mg^{2+} were considered to be originated from the crustal source. Both of the EF_{sea} for SO_4^{2-} and NO_3^- showed significantly spatial variability and they presented the higher ones in YRD and SB

(significantly higher than 1) (Fig. 8a-b), which suggested that both of the ions were not mainly sourced from the sea source. However, EF_{sea} for SO_4^{2-} in some cities such as Nujiang (0.92) and Nanchong (0.81) were lower than 1. It was assumed that the Indian monsoon played an important role on the wet deposition of SO_4^{2-} (Gu et al., 2016). Except SO_4^{2-} and NO_3^-, EF_{sea} for other ions showed relatively uniform distribution at a national scale. EF_{sea} for NH_4^+, F^-, Ca^{2+}, K^+, and Mg^{2+} in most of the cities were higher than 1 (Fig. 8c and S1), indicating the effects of anthropogenic source or crustal source. The EF_{sea} for Cl^- presented the lower value in many coastal cities such as Beihai (0.53) and Haikou (0.52), while they were significantly higher than 1 in some inland cities such as Daqing (13.11). The spatial variability of EF_{sea} for Cl^- confirmed the spatial difference of Cl^-/Na^+ between coastal cities and inland ones mentioned above. Compared with EF_{sea}, the EF_{soil} of ions generally displayed remarkably spatial variation. The EF_{soil} of SO_4^{2-}, NO_3^-, F^-, and Cl^- showed notably higher values in SEC, implicating the effects of industrial activity (Fig. 8a-b and S2a-b). The EF_{soil} of NH_4^+ presented markedly higher value in the eastern region of Inner Mongolia and Heilongjiang province such as Hegang (325.69) (Fig. 8c) because intensive grazing was beneficial to the NH_3 emission (Kobbing et al., 2014). It was interesting to note that the EF_{soil} of Na^+ showed higher value in some cities around Qinghai Lake and the evaporation of salt lake could contribute to the higher EF_{soil} of Na^+ (Fig. S2c). The EF_{soil} of crustal ions such as Mg^{2+} and K^+ in NWC were close to 1, reflecting the contributions of dust events and soils (Fig. S2e-f).

Based on the EF_{sea} and EF_{soil}, the estimated SSF, CF, and AF of ions are depicted in Fig. 9, S3, and S4. The mean SSF values of NO_3^-, F^-, Ca^{2+}, NH_4^+, Mg^{2+}, K^+, SO_4^{2-}, Cl^-, and Na^+ were 0%, 0.02%, 0.06%, 0.10%, 2.94%, 4.88%, 13.85%, 88.31%, and 100%, respectively. The average CF values of NH_4^+, NO_3^-, Cl^-, F^-, SO_4^{2-}, Na^+, K^+, Mg^{2+}, and Ca^{2+} reached 0.01%, 0.02%, 0.59%, 10.04%,

19.50%, 35.34%, 95.12%, 97.06%, and 99.94%, respectively. The AF value was considered to be the contribution ratio of each ion except SSF and CF. The AF values of Ca^{2+}, K^+, Mg^{2+}, Na^+, Cl^-, SO_4^{2-}, F^-, NH_4^+, and NO_3^- reached 0%, 0%, 0%, 0%, 11.10%, 66.65%, 89.94%, 99.89%, and 99.98%, respectively. The results suggested that NO_3^-, SO_4^{2-}, NH_4^+, and F^- were mainly sourced from anthropogenic activities based on minor SSF and CF. It was well documented that the combustion of fossil fuels, iron and steel industrial emission, and vehicle exhaust were main sources of SO_4^{2-} and NO_3^- across China (Song et al., 2006; Yang et al., 2016). In the present study, the AF values of NO_3^- in all of cities were higher than 90%, and those of SO_4^{2-} in half of the cities were higher than 60%. Besides, the utility of nitrogen fertilization, and human and livestock excretions were treated as the main source of NH_4^+ emission over China (Cao et al., 2009). Herein, 82.5% of cities across China showed the higher AF value of NH_4^+ (> 90%). Ca^{2+}, K^+, and Mg^{2+} were mainly derived from crustal origin based on the high CF values. Although the K^+ concentration in the fine particles was usually sourced from biomass burning, the component in the coarse particles generally resulted from the soil erosion and dust re-suspension (Cao et al., 2009). The higher CF values of K^+ in most of cities in China such as Aksu (Xinjiang autonomous region) and Bayin (Gansu province) suggested that the wet deposition has become the main removal mechanism for the K^+ in the coarse particles (Lim et al., 1991). The Na^+ and Cl^- ions were mainly originated from sea source because they were main components of sea-salt and sea-spray aerosol (Prather et al., 2013), which was also supported by the higher SSF value.

At a spatial scale, the highest AF values of NO_3^-, SO_4^{2-}, NH_4^+, and F^- were mainly concentrated on East China and SWC (Fig. 9a-c, S3a-c), which was similar to the spatial variation of population. The emissions of aerosols and their precursors released by human activities were mainly

concentrated on East China (Fu and Chen 2016), thereby leading to high AF values of these secondary ions. Indeed, many cities in NC such as Handan and Shijiazhuang showed the higher AF value, which revealed the effects of power plant, non-ferrous smelting, and oral mining. The SSF value of Cl^- exhibited high value in Xinjiang and Qinghai province (i.e., Altay and Haibei), SWC (i.e., Chengdu and Guangan) (Fig. S3d-e), and some coastal cities (i.e., Ningbo and Shanghai). The higher SSF values of Cl^- in SWC and coastal cities of East China were mainly controlled by Indian monsoon and East Asia monsoon driven atmospheric transport, respectively (Gu et al., 2016). However, it was assumed that the higher SSF value of Cl^- in the region close to Qinghai Lake could be linked to the evaporation of saline (Bian et al., 2017). However, the relatively higher CF value of Cl^- was centered on Ningxia autonomous region and Shaanxi province, which was frequently exposed of Aeolian dust especially under the process of wind erosion (Lyu et al., 2017). As the typical crustal ions, K^+ and Mg^{2+} in the most regions of China generally showed high CF values, especially in some cities of SWC (i.e., Guiyang, Zunyi, Zhaotong) (Fig. S4a-d). It was supposed that the severe soil erosion and loss, and rocky desertification frequently observed in Yungui Plateau contributed to the higher CF value in this region (Jiang et al., 2014). The SSF of K^+ and Mg^{2+} showed high values in some coastal cities (i.e., Sanya and Ningbo), and some cities of NWC such as Haibei (Qinghai). The evaporation of salt in East China Sea and Qinghai Lake could play a vital role on the K^+ and Mg^{2+} in these areas (Bian et al., 2017).

It should be noted that the geochemical index method showed some uncertainties for the estimation of SSF, CF, and AF. First of all, the background values of Na^+ in the sea and Ca^{2+} in the soil displayed the higher uncertainty, which varied significantly with the study areas. Unfortunately, the background values of Na^+ and Ca^{2+} over China were absent. Besides, the source classification

might be not very accurate because many other sources such as forest fire, volcanic eruption were ignored.

3.4.2 The FA-MLR analysis

In order to enhance the reliability of source identification, the FA method was also utilized to identify the source of chemical compositions in the precipitation. The FA results of four seasons are summarized in Tab. 3. Three principal components were extracted from the rainwater samples, all of which explained 85.6% of the total variance. The Kaiser-Meyer-Olkin indicator (0.85) was higher than 0.7, suggesting that three factors extracted in the present study was reasonable. Factor 1 grouped NO_3^- , F^-, NH_4^+, and SO_4^{2-}, accounting for 52.3% of the variance, which was generally associated with dense anthropogenic activities (Nayebare et al., 2016; Zhang et al., 2017b). Factor 2 displayed high loadings of Na^+ and Cl^-, indicating the effects of sea-salt and sea-spray aerosol (Gupta et al., 2015). The result was also in good agreement with the high SSF value of Na^+ and Cl^- supported by geochemical index method. Factor 3 occupied 9.54% of the total variance and was dominated by Ca^{2+}, Mg^{2+}, and K^+. The former two ions were considered to be the important indicators of crustal origin or windblown dust source, which were commonly stored in soils and dusts (Kchih et al., 2015). K^+ was also observed in urban fugitive dusts, although it was generally considered as an important fingerprint of biomass burning (Shen et al., 2016). As a whole, the result of FA was in coincident with that obtained from the EF and geochemical index method.

Although the key origins were isolated via the FA method, the contribution ratio of these sources to the water-soluble ions were still unknown. Thus, the FA-MLR method was further applied to quantify the contribution ratio of several sources to these ions in the 320 cities over China (Fig. 10a-d). In four seasons, the mean contributions of the anthropogenic source (NO_3^-, SO_4^{2-}, NH_4^+, and

744 F^-: 79.10%, 46.12%, 82.40%, and 71.02%) were significantly higher than those of sea source
745 (13.76%, 31.71%, 11.09%, and 11.52%) and crustal origin (7.14%, 22.17%, 6.52%, and 17.46%)
746 for NO_3^-, SO_4^{2-}, NH_4^+, and F^-. Nevertheless, the contribution ratio was in the order of crustal origin
747 (K^+, Ca^{2+}, and Mg^{2+}: 77.44%, 82.17%, and 70.51%) > anthropogenic source (13.91%, 10.20%, and
748 18.36%) > sea source (8.65%, 7.64%, and 11.14%) for K^+, Ca^{2+}, and Mg^{2+}. The sea source was the
749 dominant factor for the accumulation of Na^+ and Cl^- in the rainwater, followed by the crustal origin
750 and the anthropogenic source. In addition, the contribution ratios of three sources showed the slight
751 variation in different seasons (Fig. 10). For instance, the contribution ratio of sea source to most
752 inorganic ions especially Na^+ and Cl^- displayed the highest one in summer, followed by ones in
753 spring and autumn, and the lowest one in winter because the intense evaporation of sea salt in
754 summer was inclined to release more ions to the atmosphere (Teinilä et al., 2014). The contribution
755 ratio of anthropogenic activities presented the notable increase from summer to winter for SO_4^{2-}
756 because of dense coal combustion (20 kg coal/m^2) for domestic heating in winter (Zhao et al., 2016).
757 3.5 The deposition flux of the water-soluble ions and their key factors
758 At a national scale, the annually mean deposition fluxes of NO_3^-, Cl^-, Ca^{2+}, K^+, F^-, NH_4^+, Mg^{2+},
759 SO_4^{2-}, and Na^+ over China were 13.25, 8.44, 13.80, 2.49, 1.15, 5.90, 2.27, 33.41, and 4.39 kg ha^{-1}
760 yr^{-1} during 2011-2016. The deposition fluxes of NO_3^-, Ca^{2+}, K^+, NH_4^+, and Na^+ increased from 13.67
761 to 14.83 kg ha^{-1} yr^{-1}, 13.32 to 16.99 kg ha^{-1} yr^{-1}, 2.47 to 2.79 kg ha^{-1} yr^{-1}, 5.21 to 6.48 kg ha^{-1} yr^{-1},
762 and 4.17 to 5.74 kg ha^{-1} yr^{-1} from 2011 to 2013, respectively. However, they decreased to 13.65,
763 11.01, 2.52, 5.90, and 3.69 kg ha^{-1} yr^{-1} in 2016. The wet deposition fluxes of F^- and Mg^{2+} over China
764 decreased from 1.27 to 0.96 kg ha^{-1} yr^{-1} and 2.76 to 1.85 kg ha^{-1} yr^{-1} during 2012-2014, respectively.
765 However, they began to increase slightly to 1.17 and 2.15 in 2016, respectively. The wet deposition

766 fluxes of Cl^- and SO_4^{2-} showed gradual decrease from 9.80 and 38.87 kg ha^{-1} yr^{-1} to 8.09 and 26.54
767 kg ha^{-1} yr^{-1} during 2011-2016, respectively. On average, the wet deposition flux of NO_3^- were higher
768 by 2.25 times than that of NH_4^+, which was in contrast to the results of the dry deposition reported
769 by Xu et al. (2015). All of the water-soluble ions showed the highest wet deposition fluxes in
770 summer, followed by ones in spring and autumn, and the lowest ones in winter, which was probably
771 attributed by the high washout effect due to rain in summer (Jia et al., 2014). Based on the results
772 of the correlation analysis, the precipitation showed the significant relationship with the deposition
773 fluxes of the water-soluble ions ($p < 0.05$). In addition, the wet deposition fluxes of the water-soluble
774 ions showed the significantly spatial variation, which were in good agreement with the spatial
775 distribution of the water-soluble ion concentrations except Ca^{2+} (Fig. S5).

776 In order to determine the dominant factors affecting the wet deposition fluxes of the water-
777 soluble ions across China, GDP, GIP, TEC, N fertilizer use, vehicle ownership, UGS, dust days,
778 many meteorological factors (i.e., T_{max}, T_{min}, WS), and air pollutants (i.e., SO_2 and NO_2) were
779 introduced as the explanatory variables. The SR analysis results are depicted in Tab. 4. GIP, vehicle
780 ownership, NO_2, T_{min}, and wind speed served as the key factors affecting apparently the wet
781 deposition of NO_3^- at a national scale. The atmospheric emission of NO_x from coal-fired power
782 plants was estimated about 7489.6 kt in 2010, although many newly built power plants were
783 equipped with advanced low NO_x burner (LNB) systems (Tian et al., 2013). Zhang et al. (2014)
784 estimated that NO_x from vehicle emissions reached 4570 kt in 2008, which was considered as the
785 second NO_x source only to industrial activities. The NO_x released from anthropogenic activity could
786 enhance the NO_2 concentration in the ambient air, which could be also transformed to NO_3^- via
787 oxidation in the atmosphere, especially under the condition of high temperature and low WS (Zhang

et al., 2016). The wet deposition of NH_4^+ were affected by N fertilizer use, UGS, and NO_2 over China. Russel et al. (1998) recommended early that NH_4^+ in the precipitation was most likely derived from the N fertilizer use via an isotope techniques coupled with back trajectory analysis. Besides, Teng et al. (2017) demonstrated that the emission from UGS was identified to contribute to the atmospheric NH_3 significantly during 60% of the sampling times, which could increase the NH_4^+ concentration in the precipitation due to the photochemical reaction. The wet deposition flux of SO_4^{2-} was closely associated with TEC in the 320 cities of China, respectively. It was supposed that the SO_2 emission were dependent on the use of coal and petroleum (Lu et al., 2010). While terrestrial petroleum emissions have declined in recent years, the emissions from international shipping have offset the decrease of terrestrial petroleum (Smith et al., 2011). In the present study, the deposition of some crustal ions were linked to the dust days because they were mainly derived from the dust storm or soil (Deshmukh et al., 2011; Zhang et al., 2011). The F^-deposition was associated with GIP due to the contributions of the coal-fired power plant fly ash and industrial raw material (Kong et al., 2011).

The GWR method was used to calculate the local regression coefficients in order to determine the dominant factor affecting the deposition of the water-soluble ions at the regional scale (Fig. 11 and S6). The mean R^2 of GWR method was 0.50 over China, and the p value was lower than 0.05, which suggested that the GWR method could be applicable to the study.The local regression coefficient of dust days for crustal ions including Ca^{2+}, Cl^-, K^+, and Mg^{2+} increased from SEC to NWC (Fig. S6a-e), suggesting that dust days played a significant role on the crustal ions in NWC due to high intensity of dust deposition and extremely high WS (Zhang et al., 2017a). The influence of GIP on the F^- and NO_3^- increased from West China to East China, and displayed the higher value

in some cities of YRD (i.e., Shanghai, Hangzhou) because many coal-fired power plants, cement plants, and municipal solid waste incineration plants were located in YRD (Hua et al., 2016; Tian et al., 2012; Tian et al., 2014) (Fig. S6f and 11a). The influence of N fertilizer use on NH_4^+ was concentrated on some cities of NEC such as Jiamusi (Heilongjiang province) (Fig. 11b-c), Harbin (Heilongjiang province), Changchun (Jilin province) because the largest commodity grain base were located in Heilongjiang and Jilin province, leading to the higher N fertilizer use (Cheng and Zhang, 2005). In contrast to the effects of GIP, the TEC influence increased gradually from SEC to NWC, and showed the highest value in Xinjiang autonomous region (i.e., Altay) (Fig. 11d). It has been demonstrated that an inverted U-shaped curve (Environment Kuznets Curve) between per capita GDP and energy consumption was generally observed during the development of economy (Song et al., 2013; Yang et al., 2017). The Environment Kuznets Curve denoted that the energy consumption displayed positive relationship with per capita GDP in the early stage of development. However, the positive relationship tended to transform into the negative relevance with the development of economy because the reliance on the energy-intensive industries would be reduced in the developed stage (Yang et al., 2017). It was assumed that Xinjiang autonomous region kept at the early stage of the inverted-U curve and largely rested on the energy-intensive industries as the less-developed province (Yang et al., 2017). However, some developed provinces in SEC such as Zhejiang and Jiangsu have sped up structural transformation of the economy and reduce the reliance on the heavy industries. The influence of UGS and vehicle ownership peaked in Shandong province (i.e., Qingdao, Jinan) and YRD (i.e., Shanghai, Hangzhou) (Fig. 11e-f). It was supposed that the UGS and vehicle ownership in these cities showed higher values among all of the 320 cities (National Bureau of Statistics of China). Apart from the effects of socioeconomic factors, the

meteorological factors also played significant roles on NO_3^-. The influences of air temperature and WS both increased from East China to West China, and showed the highest values in Xinjiang province (Fig. 11g-h). Zhang et al. (2017a) demonstrated that the strong dust events along with high WS contributed to the neutralization of NO_3^-, although the NO_2 concentrations in some cities of Xinjiang province were significantly higher than other regions of China.

4. Conclusions

This study newly reported spatiotemporal variation of nine water-soluble ions in the precipitation across the whole China during 2011-2016. The mean pH and EC values varied significantly compared with those during 1980-2000 because the implementation of special air pollution control measures have mitigated the air pollution in China. The concentrations of Na^+, NO_3^-, and SO_4^{2-} increased from 7.26 ± 2.51, 11.56 ± 3.71, and 33.73 ± 7.59 μeq/L to 11.04 ± 4.64, 13.59 ± 2.63, and 41.95 ± 8.64 μeq/L during 2011 and 2014, while they decreased from the highest ones in 2014 to 9.75 ± 2.89, 12.29 ± 4.02, and 30.57 ± 7.43 μeq/L in 2016, respectively. The concentrations of Ca^{2+}, NH_4^+, and Mg^{2+} increased by 86.26%, 178.50%, and 19.71% from 2011 to 2013, whereas they decreased from 58.84 ± 10.31, 41.33 ± 10.26, and 10.49 ± 3.07 in 2013 to 31.20 ± 8.48, 18.13 ± 4.84, and 8.93 ± 2.92 μeq/L in 2016, respectively. The concentration of F^- decreased linearly by 5.58%/yr during 2012-2016. The mean concentrations of SO_4^{2-}, NO_3^- and F^- showed the highest values in winter, followed by ones in spring and autumn, and the lowest ones in summer. It was supposed that the dense anthropogenic activities such as domestic combustion for heating and adverse meteorological conditions. The crustal ions (Ca^{2+}, Mg^{2+}, and K^+) peaked in spring and summer, suggesting the contributions of fugitive dusts. The Na^+ and Cl^- were markedly affected by evaporation of sea salt. All of the water-soluble ions in the precipitation exhibited notably spatial

variability. The secondary ions (SO_4^{2-}, NO_3^- and NH_4^+), and F^- peaked in YRD (i.e., Changzhou, Hangzhou, and Nanjing) owing to the intensive energy consumption and industrial activities. The higher S content in the coal and unfavorable diffusion conditions contributed to the higher concentrations of secondary ions in SB (i.e., Chengdu, Leshan, and Dazhou). The crustal ions and sea-salt ions showed the highest concentrations in semi-arid regions (i.e., Guyuan, Jiayuguan) and coastal cities (i.e., Qingdao, Lianyungang), respectively.

The EF method, geochemical index method, and FA-MLR method consistently suggested that NO_3^- , F^-, NH_4^+, and SO_4^{2-} were dominated by anthropogenic activities. However, the Na^+ and Cl^- were closely associated with sea-salt aerosol. Ca^{2+}, Mg^{2+}, and K^+ were mostly derived from crustal source. The results of SR analysis and GWR method implied that GIP, TEC, vehicle ownership, and N fertilizer use were main factors for SO_4^{2-}, NO_3^-, NH_4^+, and F^- in the precipitation. However, the crustal ions were significantly affected by dust events. The correlation between influential factors and the ions in the wet deposition showed significantly spatial variability. The influence of dust days on the crustal ions increased from SEC to NWC, whereas the influence of socioeconomic factors on secondary ions showed the highest value in East China.

The present study validate the model estimations of the water-soluble ions deposition at a national scale, and provide the fundamental data for the prevention and control of acid deposition and air pollution. However, there were several plausible contributors to the uncertainty. First of all, the monitoring sites were distributed unevenly and relatively scarce sites were located in Northwest China. Moreover, the limited independent variables were included into the models. Thus, further studies were required to establish more representative monitoring sites and incorporate more variables to reduce the uncertainty associated with the ions deposition.

Author contributions

Rui Li analyzed the data and wrote the manuscript. Lulu Cui, Yilong Zhao, Ziyu Zhang, Tianming Sun, Junlin Li, Wenhui Zhou, Ya Meng, and Kan Huang organized the campaign and analyzed data. Hongbo Fu revised the manuscript.

Acknowledgements

This work was supported by National Key R&D Program of China (2016YFC0202700), National Natural Science Foundation of China (Nos. 91744205, 21777025, 21577022, 21177026), International cooperation project of Shanghai municipal government (15520711200), and Marie Skłodowska-Curie Actions (690958-MARSU-RISE-2015). The meteorological data are avaiable at http://data.cma.cn/. The socioeonomic data are collected from http://www.stats.gov.cn/.

References

Abed, A.M., Kuisi, M.A., Khair, H.A.: Characterization of the Khamaseen (spring) dust in Jordan, Atmos. Environ. 43, 2868-2876, https://doi.org/10.1016/j.atmosenv.2009.03.015, 2009.

AlKhatib, M. and Eisenhauer, A.: Calcium and strontium isotope fractionation during precipitation from aqueous solutions as a function of temperature and reaction rate; II. Aragonite. 209, 320-342, 2017.

Al-Khashman, O. A.: Study of chemical composition in wet atmospheric precipitation in Eshidiya area, Jordan, Atmos. Environ. 39(33), 6175-6183, https://doi.org/10.1016/j.atmosenv.2005.06.056, 2005.

Allen, H. M., Draper, D.C., Ayres, B.R., Ault, R., Bondy, A., Takahama, S., Modini, R.L., Baumann, K., Edgerton, E., and Knote, C.: Influence of crustal dust and sea spray supermicron particle concentrations and acidity on inorganic NO_3^- aerosol during the 2013 Southern Oxidant and Aerosol Study, Atmos. Chem. Phys., 15(18), 10669-10685, https://www.atmos-chem-phys.net/15/10669/2015/, 2015.

Aloisi, I., G. Cai, C. Faleri, L. Navazio, D. Serafini-Fracassini, and S. Del Duca.: Spermine regulates pollen tube growth by modulating Ca^{2+}-dependent actin organization and cell wall structure, Front Plant Sci, 8, 1701, 2017.

Antony Chen, L. W., B. G. Doddridge, R. R. Dickerson, J. C. Chow, P. K. Mueller, J. Quinn, and W. A. Butler.: Seasonal variations in elemental carbon aerosol, carbon monoxide and sulfur dioxide: Implications for sources, Geophys. Res. Lett., 28(9), 1711-1714, https://doi.org/10.1029/2000GL012354, 2001.

Arimoto, R., R. Duce, D. Savoie, J. Prospero, R. Talbot, J. Cullen, U. Tomza, N. Lewis, and B. Ray.: Relationships among aerosol constituents from Asia and the North Pacific during PEM - West A, J. Geophys. Res., 101(D1), 2011-2023, https://doi.org/10.1029/95JD01071, 1996.

Bao, G., Q. Ao, Q. Li, Y. Bao, Y. Zheng, X. Feng, and X. Ding.: Physiological Characteristics of Medicago sativa L. in Response to Acid Deposition and Freeze-Thaw Stress, Water Air Soil Poll., 228(9),

376, 2017.

Balasubramanian, R., Victor, T., Chun, N.: Chemical and statistical analysis of precipitation in Singapore. Water Air Soil Poll. 130, 451-456, 2001.

Baumbach, G., Vogt, U.: Experimental determination of the effect of mountain-valley breeze circulation on air pollution in the vicinity of Freiburg. Atmos. Environ. 33, 4019-4027, https://doi.org/10.1016/S1352-2310(99)00143-0, 1999.

Beniston.: Environmental change in mountains and uplands, 2016.

Bian, S., D. Li, D. Gao, J. Peng, Y. Dong, and W. Li.: Hydrometallurgical processing of lithium, potassium, and boron for the comprehensive utilization of Da Qaidam lake brine via natural evaporation and freezing, Hydrometallurgy, 173, 80-83, 2017.

Bowden, R. D., E. Davidson, K. Savage, C. Arabia, and P. Steudler.: Chronic nitrogen additions reduce total soil respiration and microbial respiration in temperate forest soils at the Harvard Forest, Forest Ecol Manag., 196(1), 43-56, 2004.

Cao, Y.-Z., S. Wang, G. Zhang, J. Luo, and S. Lu.: Chemical characteristics of wet precipitation at an urban site of Guangzhou, South China, Atmos. Res., 94(3), 462-469, https://doi.org/10.1016/j.atmosres.2009.07.004, 2009.

Cabello, M., Orza, J.A.G., Duenas, C., Liger, E., Gordo, E., Canete, S.: Back-trajectory analysis of African dust outbreaks at a coastal city in southern Spain: Selection of starting heights and assessment of African and concurrent Mediterranean contributions, Atmos. Environ., 140, 10-21, https://doi.org/10.1016/j.atmosenv.2016.05.047, 2016.

Chen, J., C. Li, Z. Ristovski, A. Milic, Y. Gu, M. S. Islam, S. Wang, J. Hao, H. Zhang, and C. He.: A review of biomass burning: Emissions and impacts on air quality, health and climate in China, Sci. Total

Environ., 579, 1000-1034, https://doi.org/10.1016/j.scitotenv.2016.11.025, 2017a.

Chen, J., G. Liu, Y. Kang, B. Wu, R. Sun, C. Zhou, and D. Wu.: Atmospheric emissions of F, As, Se, Hg, and Sb from coal-fired power and heat generation in China, Chemosphere, 90(6), 1925-1932, https://doi.org/10.1016/j.chemosphere.2012.10.032, 2013.

Chen, P., T. Wang, X. Lu, Y. Yu, M. Kasoar, M. Xie, and B. Zhuang.: Source apportionment of size-fractionated particles during the 2013 Asian Youth Games and the 2014 Youth Olympic Games in Nanjing, China, Sci. Total Environ., 579, 860-870, https://doi.org/10.1016/j.scitotenv.2016.11.014, 2017b.

Chen, Y., B. Luo, and S.-d. Xie.: Characteristics of the long-range transport dust events in Chengdu, Southwest China, Atmos. Environ., 122, 713-722, https://doi.org/10.1016/j.atmosenv.2015.10.045, 2015.

Cheng, Y.-q., and P. Zhang.: Regional patterns changes of Chinese grain production and response of commodity grain base in northeast China, Scientia Geographica Sinica, 25(5), 514, 2005.

Cheng, Y., G. Engling, K.-b. He, F.-k. Duan, Z.-y. Du, Y.-l. Ma, L.-l. Liang, Z.-f. Lu, J.-m. Liu, and M. Zheng.: The characteristics of Beijing aerosol during two distinct episodes: Impacts of biomass burning and fireworks, Environ. Pollut., 185, 149-157, https://doi.org/10.1016/j.envpol.2013.10.037, 2014.

Chen, Z.J., Chen, C.X., Liu, Y.Q., Lin, Z.S.: The background values and characteristics of soil elements in Fujian province. Environ. Monit. China, 8, 107-110, 1992.

Cong, Z., S. Kang, and K. Kawamura (2016), The long-range transport of atmospheric aerosols from South Asia to Himalayas, paper presented at EGU General Assembly Conference Abstracts.

Clemens, S.: Toxic metal accumulation, responses to exposure and mechanisms of tolerance in plants, 88, 1707-1719, 2006.

Dai, S., and D. Ren.: Fluorine concentration of coals in China-an estimation considering coal reserves,

Fuel, 85(7), 929-935, 2006.

Deshmukh, D. K., M. K. Deb, Y. I. Tsai, and S. L. Mkoma.: Water soluble ions in $PM_{2.5}$ and PM_1 aerosols in Durg city, Chhattisgarh, India, Aerosol Air Qual. Res, 11, 696-708, 10.4209/aaqr.2011.03.0023, 2011.

Ding, X., L. Kong, C. Du, A. Zhanzakova, H. Fu, X. Tang, L. Wang, X. Yang, J. Chen, and T. Cheng.: Characteristics of size-resolved atmospheric inorganic and carbonaceous aerosols in urban Shanghai, Atmos. Environ., 167, 625-641, https://doi.org/10.1016/j.atmosenv.2017.08.043, 2017.

Dong, Z.W., Kang, S.C., Guo, J.M., Zhang, Q.G., Wang, X.J., Qi, D.H.: Composition and mixing states of brown haze particle over the Himalayas along two transboundary south-north transects, Atmos. Environ., 156, 24-35, https://doi.org/10.1016/j.atmosenv.2017.02.029, 2017.

Driscoll, C. T., K. M. Driscoll, M. J. Mitchell, and D. J. Raynal.: Effects of acidic deposition on forest and aquatic ecosystems in New York State, Environ. Pollut., 123(3), 327-336, https://doi.org/10.1016/S0269-7491(03)00019-8, 2003.

Du, E.Z., Vries, W.D., Galloway, J.N., Hu, X.Y., Fang, J.Y.: Changes in wet nitrogen deposition in the United States between 1985 and 2012, Environ. Res. Lett., 9, 095004, https://doi.org/10.1088/1748-9326/9/9/095004, 2014.

Emmett, B.: The impact of nitrogen on forest soils and feedbacks on tree growth, in Forest Growth Responses to the Pollution Climate of the 21st Century, edited, pp. 65-74, Springer, 1999.

Engelbrecht, P. J., Moosmüller, H., Pincock, S., Jayanty, R.K.M., Lersch, T., Casuccio, G.: Technical note: Mineralogical, chemical, morphological, and optical interrelationships of mineral dust re-suspensions. Atmos. Chem. Phys. 16, 10809–10830, https://www.atmos-chem-phys.net/16/10809/2016/, 2016.

Fornaro, A., Gutz, I.G.R.: Wet deposition and related atmospheric chemistry in the São Paulo metropolis,

Brazil: part 2-contribution of formic and acetic acids. Atmos. Environ. 37, 117-128, https://doi.org/10.1016/S1352-2310(02)00885-3, 2003.

Fu, H., G. Shang, J. Lin, Y. Hu, Q. Hu, L. Guo, Y. Zhang, and J. Chen.: Fractional iron solubility of aerosol particles enhanced by biomass burning and ship emission in Shanghai, East China, Sci. Total Environ., 481, 377-391, https://doi.org/10.1016/j.scitotenv.2014.01.118, 2014.

Fu, H.B., Chen, J.M.: Formation, features and controlling strategies of severe haze-fog pollutions in China, Sci. Total Environ., 578, 121-138, https://doi.org/10.1016/j.scitotenv.2016.10.201, 2016.

Garland, J.A.: Dry and wet removal of sulphur from the atmosphere, Sulfur in the Atmosphere, 349-362, 1978.

Gerson, J. R., C. T. Driscoll, and K. M. Roy.: Patterns of nutrient dynamics in Adirondack lakes recovering from acid deposition, Ecol. Appl., 26(6), 1758-1770, 2016.

Glavas, S., Moschonas, N.: Origin of observed acidic–alkaline rains in a wet-only precipitation study in a Mediterranean coastal site, Patras, Greece. Atmos. Environ. 36, 3089–3099, https://doi.org/10.1016/S1352-2310(02)00262-5, 2002.

Gottwald, M., Bovensmann, H.: SCIAMACHY: Exploring the Changing Earth's Atmosphere, first ed. Springer (ISBN 978-9-481-9895-5), 2011.

Grythe, H., J. Ström, R. Krejci, P. Quinn, and A. Stohl.: A review of sea-spray aerosol source functions using a large global set of sea salt aerosol concentration measurements, Atmos. Chem. Phys., 14(3), 1277, https://www.atmos-chem-phys.net/14/1277/2014/, 2014.

Gu, J., Pitz, M., Schnelle-Kreis, J., Diemer, J., Reller, A., Zimmermann, R., Soentgen, J., Stoelzel, M., Wichmann, H.E., Peters, A., Cyrys, J.: Source apportionment of ambient particles: comparison of positive matrix factorization analysis applied to particle size distribution and chemical composition data.

Atmos. Environ. 45, 1849-1857, https://doi.org/10.1016/j.atmosenv.2011.01.009, 2011.

Gu, Y., H. Liao, and J. Bian.: Summertime nitrate aerosol in the upper troposphere and lower stratosphere over the Tibetan Plateau and the South Asian summer monsoon region, Atmos. Chem. Phys., 16(11), 6641-6663, https://doi.org/10.5194/acp-16-6641-2016, 2016.

Gupta, D., H.-J. Eom, H.-R. Cho, and C.-U. Ro.: Hygroscopic behavior of NaCl-$MgCl_2$ mixture particles as nascent sea-spray aerosol surrogates and observation of efflorescence during humidification, Atmos. Chem. Phys., 15(19), 11273-11290, https://doi.org/10.5194/acp-15-11273-2015, 2015.

Hao, G.J., Zhou, J.Q., Fang, H.L.: Applicability of AB-DTPA method for determining the available content of multi-element in typical soils in China, Acta Agr. Shanghai (in Chinese), 32, 100-107, 2016.

Hua, S., H. Tian, K. Wang, C. Zhu, J. Gao, Y. Ma, Y. Xue, Y. Wang, S. Duan, and J. Zhou.: Atmospheric emission inventory of hazardous air pollutants from China's cement plants: Temporal trends, spatial variation characteristics and scenario projections, Atmos. Environ., 128, 1-9, https://doi.org/10.1016/j.atmosenv.2015.12.056, 2016.

Hunová, I., Maznová, J., Kurfürst, P.: Trends in atmospheric deposition fluxes of sulphur and nitrogen in Czech forests, Environ. Pollut., 184, 668-675, https://doi.org/10.1016/j.envpol.2013.05.013, 2014.

Ito, M., Mitchell, M., Driscoll, C.T.: Spatial patterns of precipitation quantity and chemistry and air temperature in the Adirondack region of New York. Atmos. Environ. 36, 1051–1062, https://doi.org/10.1016/S1352-2310(01)00484-8, 2002.

Jia, Y., G. Yu, N. He, X. Zhan, H. Fang, W. Sheng, Y. Zuo, D. Zhang, and Q. Wang.: Spatial and decadal variations in inorganic nitrogen wet deposition in China induced by human activity, Scientific Reports, 4, https://doi.org/10.1038/srep03763, 2014.

Jiang, Z., Y. Lian, and X. Qin.: Rocky desertification in Southwest China: impacts, causes, and

restoration, Earth-Science Reviews, 132, 1-12, https://doi.org/10.1016/j.earscirev.2014.01.005, 2014.

Kang, Y., M. Liu, Y. Song, X. Huang, H. Yao, X. Cai, H. Zhang, L. Kang, X. Liu, and X. Yan.: High-resolution ammonia emissions inventories in China from 1980 to 2012, Atmos. Chem. Phys., 16(4), 2043-2058, https://doi.org/10.5194/acp-16-2043-2016, 2016.

Kang, L.T., Huang, J.P., Chen, S.Y., Wang, X.: Long-term trends of dust events over Tibetan Plateau during 1961–2010, Atmos. Environ., 125, 188-198, https://doi.org/10.1016/j.atmosenv.2015.10.085, 2016.

Kabatas, B., Unal, A., Pierce, R.B., Kindap, T., Pozzoli, L.: The contribution of Saharan dust in PM_{10} concentration levels in Anatolian Peninsula of Turkey, Sci. Total Environ., 488-489, 413-421, https://doi.org/10.1016/j.scitotenv.2013.12.045, 2014.

Kchih, H., C. Perrino, and S. Cherif.: Investigation of desert dust contribution to source apportionment of PM_{10} and $PM_{2.5}$ from a southern Mediterranean coast, Aerosol Air Qual. Res. 15(2), 454-464, 10.4209/aaqr.2014.10.0255, 2015.

Keene, W. C., Pszenny, A. A. P., Galloway, J. N., and Hawley, M. E.: Sea-salt corrections and interpretation of constituent ratios in marine precipitation, J. Geophys. Res.-Atmos., 91, 6647–6658, https://doi.org/10.1029/JD091iD06p06647, 1986.

Kong, S., Y. Ji, B. Lu, L. Chen, B. Han, Z. Li, and Z. Bai.: Characterization of PM_{10} source profiles for fugitive dust in Fushun-a city famous for coal, Atmos. Environ., 45(30), 5351-5365, https://doi.org/10.1016/j.atmosenv.2011.06.050, 2011.

Kobbing, J.F., Patuzzi, F., Baratieri, M., Beckmann, V., Thevs, N., Zerbe, S.: Economic evaluation of common reed potential for energy production: a case study in Wuliangsuhai Lake (Inner Mongolia, China). Biomass Bioenerg. 70, 315-329, 2014.

Kulshrestha, U.C., Sarkar, A.K., Srivastava, S.S., Parashar, D.C.: Wet-only and bulk deposition studies at New Delhi (India). Water Air Soil Pollut., 85, 2137–2142, 1995.

Kuribayashi, M., T. Ohara, Y. Morino, I. Uno, J.-i. Kurokawa, and H. Hara.: Long-term trends of sulfur deposition in East Asia during 1981-2005, Atmos. Environ., 59, 461-475, https://doi.org/10.1016/j.atmosenv.2012.04.060, 2012.

Kuang, F.H., Liu, X.J., Zhu, B., Shen, J., Pan, Y., Su, M.: Wet and dry nitrogen deposition in the central Sichuan Basin of China, Atmos. Environ. 143, 39-50, https://doi.org/10.1016/j.atmosenv.2016.08.032, 2016.

Lawson, D.R., Winchester, J.W.: A standard crustal aerosol as a reference for elemental enrichment factors, Atmos. Environ. 13, 925-930, 1979.

Larssen, T., and G. Carmichael.: Acid rain and acidification in China: the importance of base cation deposition, Environ. Pollut., 110(1), 89-102, https://doi.org/10.1016/S0269-7491(99)00279-1, 2000.

Larssen, T., H. M. Seip, A. Semb, J. Mulder, I. P. Muniz, R. D. Vogt, E. Lydersen, V. Angell, T. Dagang, and O. Eilertsen.: Acid deposition and its effects in China: an overview, Environ. Sci. Poli., 2(1), 9-24, 1999.

Leng, Q.M., Cui, J., Zhou, F.W., Du, K., Zhang, L.Y., Fu, C., Liu, Y., Wang, H.B., Shi, G.M., Gao, M., Yang, F.M., He, D.Y.: Wet-only deposition of atmospheric inorganic nitrogen and associated isotopic characteristics in a typical mountain area, southwestern China, Sci. Environ. Total, 616, 55-63, https://doi.org/10.1016/j.scitotenv.2017.10.240, 2018.

Le Bolloch, O., Guerzoni, S.: Acid and alkaline deposition in precipitation on the western coast of Sardinia, Central Mediterranean (40 N, 81 E). Water Air Soil Poll. 85, 2155-2160, 1995.

Li, C.L., Kang, S.C., Zhang, Q.G., Kaspari, S.: Major ionic composition of precipitation in the Nam Co

region, Central Tibetan Plateau. Atmos. Res. 85, 351–360, https://doi.org/10.1016/j.atmosres.2007.02.006, 2007.

Li, L., Q. Tan, Y. Zhang, M. Feng, Y. Qu, J. An, and X. Liu.: Characteristics and source apportionment of $PM_{2.5}$ during persistent extreme haze events in Chengdu, southwest China, Environ. Pollut., 230, 718-729, https://doi.org/10.1016/j.envpol.2017.07.029, 2017a.

Li, R., L. Cui, J. Li, A. Zhao, H. Fu, Y. Wu, L. Zhang, L. Kong, and J. Chen.: Spatial and temporal variation of particulate matter and gaseous pollutants in China during 2014–2016, Atmos. Environ., 161, 235-246, https://doi.org/10.1016/j.atmosenv.2017.05.008, 2017b.

Li, X., L. Wang, D. Ji, T. Wen, Y. Pan, Y. Sun, and Y. Wang.: Characterization of the size-segregated water-soluble inorganic ions in the Jing-Jin-Ji urban agglomeration: Spatial/temporal variability, size distribution and sources, Atmos. Environ., 77, 250-259, https://doi.org/10.1016/j.atmosenv.2013.03.042, 2013.

Li, Y., J. Meng, J. Liu, Y. Xu, D. Guan, W. Tao, Y. Huang, and S. Tao.: Interprovincial reliance for improving air quality in China: a case study on black carbon aerosol, Environ. Sci. Technol., 50(7), 4118-4126, 10.1021/acs.est.5b05989, 10.1021/acs.est.5b05989, 2016.

Li, R., Li, J.L., Cui, L.L., Wu, Y., Fu, H.B., Chen, J.M., Chen, M.D.: Atmospheric emissions of Cu and Zn from coal combustion in China: Spatio-temporal distribution, human health effects, and short-term prediction, Environ. Pollut., 229, 724-734, https://doi.org/10.1016/j.envpol.2017.05.068, 2017.

Li, Z.Y., Wang, Z.L., Li, R.J., Xu, Q,H.: The analysis of element content in the soil of 29 provinces/municipality/autonomous region in China, Shanghai agriculture technology (in Chinese), 1992.

Li, Z., Ma, Z., vander Kuijp, T., Yuan, Z.W., Huang, L.: A review of soil heavy metal pollution from mines in China: Pollution and health risk assessment, Sci. Total Environ. 468-469, 843-853,

https://doi.org/10.1016/j.scitotenv.2018.06.068, 2014.

Lim, B., T. Jickells, and T. Davies.: Sequential sampling of particles, major ions and total trace metals in wet deposition, Atmospheric Environment. Part A. General Topics, 25(3-4), 745-762, 1991.

Link, M. F., J. Kim, G. Park, T. Lee, T. Park, Z. B. Babar, K. Sung, P. Kim, S. Kang, and J. S. Kim.: Elevated production of NH_4-NO_3 from the photochemical processing of vehicle exhaust: Implications for air quality in the Seoul Metropolitan Region, Atmos. Environ., 156, 95-101, https://doi.org/10.1016/j.atmosenv.2017.02.031, 2017.

Liu, F., S. Beirle, Q. Zhang, B. Zheng, D. Tong, and K. He.: NO_x emission trends over Chinese cities estimated from OMI observations during 2005 to 2015, Atmos. Chem. Phys., 17(15), 9261-9275, https://doi.org/10.5194/acp-17-9261-2017, 2017.

Liu, F., Q. Zhang, D. Tong, B. Zheng, M. Li, H. Huo, and K. He.: High-resolution inventory of technologies, activities, and emissions of coal-fired power plants in China from 1990 to 2010, Atmos. Chem. Phys., 15(23), 13299-13317, https://doi.org/10.5194/acp-15-13299-2015, 2015a.

Liu, Y. W., Ri, X., Wang, Y. S., Pan, Y. P., Piao, S. L.: Wet deposition of atmospheric inorganic nitrogen at five remote sites in the Tibetan Plateau, Atmos. Chem. Phys., 15, 11683-11700, https://doi.org/10.5194/acp-15-11683-2015, 2015b.

Liu, L., Zhang, X.Y., Wang, S.Q., Zhang, W.T., Lu, X.H.: Bulk sulfur deposition in China, Atmos. Environ., 135, 41-49, https://doi.org/10.1016/j.atmosenv.2016.04.003, 2016a.

Liu, P.F., Zhang, C., Mu, Y., Liu, C.T., Xue, C.Y., Ye, C., Liu, J.F., Zhang, Y.Y., Zhang, H.X.: The possible contribution of the periodic emissions from farmers' activities in the North China Plain to atmospheric water-soluble ions in Beijing, Atmos. Chem. Phys., 16, 10097-10109, https://doi.org/10.5194/acp-16-10097-2016, 2016b.

Liu, P.F., Zhang, C.L., Xue, C.Y., Mu, Y.J., Liu, J.F., Zhang, Y.Y., Tian, D., Ye, C., Zhang, H.X., Guan, J.: The contribution of residential coal combustion to atmospheric $PM_{2.5}$ in northern China during winter, Atmos. Chem. Phys., 17, 11503–11520, https://doi.org/10.5194/acp-17-11503-2017, 2017.

Liu, X., L. Duan, J. Mo, E. Du, J. Shen, X. Lu, Y. Zhang, X. Zhou, C. He, and F. Zhang.: Nitrogen deposition and its ecological impact in China: an overview, Environ. Pollut., 159(10), 2251-2264, https://doi.org/10.1016/j.envpol.2010.08.002, 2011.

Liu, X., X. Ju, Y. Zhang, C. He, J. Kopsch, and Z. Fusuo.: Nitrogen deposition in agroecosystems in the Beijing area, Agr. Ecosyst. Enviro., 113(1), 370-377, 2006.

Liu, X., Y. Zhang, W. Han, A. Tang, J. Shen, Z. Cui, P. Vitousek, J. W. Erisman, K. Goulding, and P. Christie.: Enhanced nitrogen deposition over China, Nature, 494(7438), 459, https://doi.org/10.1038/nature11917, 2013.

Lu, X., L. Y. Li, N. Li, G. Yang, D. Luo, and J. Chen.: Chemical characteristics of spring precipitation of Xi'an city, NW China, Atmos. Environ., 45(28), 5058-5063, https://doi.org/10.1016/j.atmosenv.2011.06.026, 2011.

Lu, X., Q. Mao, F. S. Gilliam, Y. Luo, and J. Mo.: Nitrogen deposition contributes to soil acidification in tropical ecosystems, Global Change Biol., 20(12), 3790-3801, https://doi.org/10.1111/gcb.12665, 2014.

Lu, Z., D. G. Streets, Q. Zhang, S. Wang, G. R. Carmichael, Y. F. Cheng, C. Wei, M. Chin, T. Diehl, and Q. Tan.: Sulfur dioxide emissions in China and sulfur trends in East Asia since 2000, Atmos. Chem. Phys., 10(13), 6311-6331, https://doi.org/10.5194/acp-10-6311-2010, 2010.

Luo, X.S., Xue, Y., Wang, Y.L., Cang, L., Xu, B., Ding, J.: Source identification and apportionment of heavy metals in urban soil profiles, Chemosphere., 127, 152-157, https://doi.org/10.1016/j.chemosphere.2015.01.048, 2015.

Lyu, X., N. Chen, H. Guo, L. Zeng, W. Zhang, F. Shen, J. Quan, and N. Wang.: Chemical characteristics and causes of airborne particulate pollution in warm seasons in Wuhan, central China, Atmos. Chem. Phys., 16(16), 10671-10687, https://doi.org/10.5194/acp-16-10671-2016, 2016.

Lyu, Y., Z. Qu, L. Liu, L. Guo, Y. Yang, X. Hu, Y. Xiong, G. Zhang, M. Zhao, and B. Liang.: Characterization of dustfall in rural and urban sites during three dust storms in northern China, 2010, Aeolian Res., 28, 29-37, 2017.

McGlade, C., Ekins, P.: The geographical distribution of fossil fuels unused when limiting global warming to 2 °C, Nature, 517, 187-190, https://doi.org/10.1038/nature14016, 2015.

Müller, W. E., E. Tolba, Q. Feng, H. C. Schröder, J. S. Markl, M. Kokkinopoulou, and X. Wang.: Amorphous Ca^{2+} polyphosphate nanoparticles regulate the ATP level in bone-like SaOS-2 cells, J. Cell Sci., 128(11), 2202-2207, 2015.

Migliavacca, D., E. Teixeira, F. Wiegand, A. Machado, and J. Sanchez.: Atmospheric precipitation and chemical composition of an urban site, Guaiba hydrographic basin, Brazil, Atmos. Environ., 39(10), 1829-1844, https://doi.org/10.1016/j.atmosenv.2004.12.005, 2005.

Mikhailova, E., M. Goddard, C. Post, M. Schlautman, and J. Galbraith.: Potential contribution of combined atmospheric Ca^{2+} and Mg^{2+} wet deposition within the continental US to soil inorganic carbon sequestration, Pedosphere, 23(6), 808-814, 2013.

National Bureau of Statistics of China, 2010-2016 (Chinese).

Négrel, P., C. Guerrot, and R. Millot.: Chemical and strontium isotope characterization of precipitation in France: influence of sources and hydrogeochemical implications, Isot. Environ. Healt., 43(3), 179-196, 2007.

Nayebare, S. R., O. S. Aburizaiza, H. A. Khwaja, A. Siddique, M. M. Hussain, J. Zeb, F. Khatib, D. O.

Carpenter, and D. R. Blake.: Chemical Characterization and Source Apportionment of $PM_{2.5}$ in Rabigh, Saudi Arabia, Aerosol Air Qual Re., 16(12), 3114-3129, 10.4209/aaqr.2015.11.0658, 2016.

Niu, H.W., He, Y.Q., Lu, X.X., Shen, J., Du, J.K., Zhang, T., Pu, T., Xin, H.J., Chang, L.: Chemical composition of precipitation in the Yulong Snow Mountain region, Southwestern China. Atmos. Res. 144, 195-206, https://doi.org/10.1016/j.atmosres.2014.03.010, 2014.

Okuda, T., T. Iwase, H. Ueda, Y. Suda, S. Tanaka, Y. Dokiya, K. Fushimi, and M. Hosoe.: Long-term trend of chemical constituents in precipitation in Tokyo metropolitan area, Japan, from 1990 to 2002, Sci. Total Environ. 339(1), 127-141, https://doi.org/10.1016/j.scitotenv.2004.07.024, 2005.

Wang, W.X., Xu, P.J.: Research Progress in Precipitation Chemistry in China, Progress in Chemistry, Z1, 2009.

Padoan, E., Ajmone-Marsan, F., Querol, X., Amato, F.: An empirical model to predict road dust emissions based on pavement and traffic characteristics, Environ. Pollut. 237, 713-720, https://doi.org/10.1016/j.envpol.2017.10.115, 2017.

Pan, Y. P., Wang, Y. S., Tang, G. Q., Du, W.: Spatial distribution and temporal variations of atmospheric sulfur deposition in Northern China: insights into the potential acidification risks, Atmos. Chem. Phys. 1675-1688, https://doi.org/10.5194/acp-13-1675-2013, 2013.

Prather, K. A., T. H. Bertram, V. H. Grassian, G. B. Deane, M. D. Stokes, P. J. DeMott, L. I. Aluwihare, B. P. Palenik, F. Azam, and J. H. Seinfeld.: Bringing the ocean into the laboratory to probe the chemical complexity of sea spray aerosol, P. Natl. Acad. Sci. USA. 110(19), 7550-7555, https://doi.org/10.1073/pnas.1300262110, 2013.

Pu, W., W. Quan, Z. Ma, X. Shi, X. Zhao, L. Zhang, Z. Wang, and W. Wang.: Long-term trend of chemical composition of atmospheric precipitation at a regional background station in Northern China, Sci. Total

Environ., 580, 1340-1350, https://doi.org/10.1016/j.scitotenv.2016.12.097, 2017.

Qiao, T., M. Zhao, G. Xiu, and J. Yu.: Seasonal variations of water soluble composition (WSOC, Hulis and WSIIs) in PM_1 and its implications on haze pollution in urban Shanghai, China, Atmos. Environ., 123, 306-314, https://doi.org/10.1016/j.atmosenv.2015.03.010, 2015.

Qiao, X., Du, J., Kota, S.H., Ying, Q., Xiao, W.Y., Tang, Y.: Wet deposition of sulfur and nitrogen in Jiuzhaigou National Nature Reserve, Sichuan, China during 2015-2016: Possible effects from regional emission reduction and local tourist activities. 233, 267-277. Environ. Pollut. 233, 267-277, https://doi.org/10.1016/j.envpol.2017.08.041, 2018.

Rao, W., G. Han, H. Tan, and S. Jiang.: Chemical and Sr isotopic compositions of precipitation on the Ordos Desert Plateau, Northwest China, Environ. Earth Sci., 74(7), 5759-5771, 2015.

Ren, D., F. Zhao, S. Dai, J. Zhang, and K. Luo.: Trace Element Geochemical in Coal, edited, Science Press, Beijing, China, 2006.

Russell, K. M., J. N. Galloway, S. A. Macko, J. L. Moody, and J. R. Scudlark.: Sources of nitrogen in wet deposition to the Chesapeake Bay region, Atmos. Environ., 32(14), 2453-2465, https://doi.org/10.1016/S1352-2310(98)00044-2, 1998.

Seinfeld, J. H.: Atmospheric Chemistry and Physics of Air Pollution John Wiley & Sons, Inc., New York, 50-51, 1986.

Shen, Z., J. Sun, J. Cao, L. Zhang, Q. Zhang, Y. Lei, J. Gao, R.-J. Huang, S. Liu, and Y. Huang.: Chemical profiles of urban fugitive dust $PM_{2.5}$ samples in Northern Chinese cities, Sci. Total Environ., 569, 619-626, https://doi.org/10.1016/j.scitotenv.2016.06.156, 2016.

Shi, C.W., Zhao, L.Z., Guo, X.B., Gao, S., Yang, J.P., Li, J.H.: The distribution characteristic and influential factors of background values for elements in Shanxi province, Agro-environmental Protection,

15, 24-28, 1996.

Shi, G.L., Liu, G.R., Peng, X., Wang, Y.N., Tian, Y.Z., Wang, W., Feng, Y.C.: A comparison of multiple combined models for source apportionment, including the PCA/MLR-CMB, UNMIX-CMB and PMF-CMB Models, Aerosol Air Qual. R., 14, 2040-2050, 2014.

Sickles II, J.E., Shadwick, D.S.: Air quality and atmospheric deposition in the eastern US: 20 years of change, Atmos. Chem. Phys., 15, 173-197, https://doi.org/10.5194/acp-15-173-2015, 2015.

Simkin, S. M., E. B. Allen, W. D. Bowman, C. M. Clark, J. Belnap, M. L. Brooks, B. S. Cade, S. L. Collins, L. H. Geiser, and F. S. Gilliam.: Conditional vulnerability of plant diversity to atmospheric nitrogen deposition across the United States, P. Natl. Acad. Sci. USA., 113(15), 4086-4091, https://doi.org/10.1073/pnas.1515241113, 2016.

Singh, A., Agrawal, M.: Acid rain and its ecological consequences. J. Environ. Biol. 29, 15-24, 2008.

Smith, S. J., J. v. Aardenne, Z. Klimont, R. J. Andres, A. Volke, and S. Delgado Arias.: Anthropogenic sulfur dioxide emissions: 1850–2005, Atmos. Chem. Phys., 11(3), 1101-1116, https://doi.org/10.5194/acp-11-1101-2011, 2011.

Song, F., Gao, Y.: Chemical characteristics of precipitation at metropolitan Newark in the US East Coast. Atmos. Environ. 43, 4903-4913, https://doi.org/10.1016/j.atmosenv.2009.07.024, 2009.

Song, H., K. Zhang, S. Piao, and S. Wan.: Spatial and temporal variations of spring dust emissions in northern China over the last 30 years, Atmos. Environ., 126, 117-127, https://doi.org/10.1016/j.atmosenv.2015.11.052, 2016.

Song, Y., Y. Zhang, S. Xie, L. Zeng, M. Zheng, L. G. Salmon, M. Shao, and S. Slanina.: Source apportionment of $PM_{2.5}$ in Beijing by positive matrix factorization, Atmos. Environ., 40(8), 1526-1537, https://doi.org/10.1016/j.atmosenv.2005.10.039, 2006.

Sun, L., L. Li, Z. Chen, J. Wang, and Z. Xiong.: Combined effects of nitrogen deposition and biochar application on emissions of N_2O, CO_2 and NH_3 from agricultural and forest soils, Soil Sci. Plant Nutr., 60(2), 254-265, 2014.

Sun, S.D., Jiang, W., Gao, W.D.: Vehicle emission trends and spatial distribution in Shandong province, China, from 2000 to 2014, Atmos. Environ., 147, 190-199, https://doi.org/10.1016/j.atmosenv.2016.09.065, 2016.

Song, M.-L., Zhang, W., Wang, S.-H.: Inflection point of environmental Kuznets curve in Mainland China. Energy Policy 57, 14-20., 2013.

Song, L., Kuang, F.H., Skiba, U., Zhu, B., Liu, X.J., Levy, P., Dore, A., Fowler, D.: Bulk deposition of organic and inorganic nitrogen in southwest China from 2008 to 2013, Environ. Pollut., 227, 157-166, https://doi.org/10.1016/j.envpol.2017.04.031, 2017.

Tai, A. P., L. J. Mickley, and D. J. Jacob.: Correlations between fine particulate matter ($PM_{2.5}$) and meteorological variables in the United States: Implications for the sensitivity of $PM_{2.5}$ to climate change, Atmos. Environ., 44(32), 3976-3984, https://doi.org/10.1016/j.atmosenv.2010.06.060, 2010.

Tao, J., L. Zhang, R. Zhang, Y. Wu, Z. Zhang, X. Zhang, Y. Tang, J. Cao, and Y. Zhang.: Uncertainty assessment of source attribution of $PM_{2.5}$ and its water-soluble organic carbon content using different biomass burning tracers in positive matrix factorization analysis-A case study in Beijing, China, Sci. Total Environ., 543, 326-335, https://doi.org/10.1016/j.scitotenv.2015.11.057, 2016.

Teinilä, K., A. Frey, R. Hillamo, H. C. Tülp, and R. Weller.: A study of the sea-salt chemistry using size-segregated aerosol measurements at coastal Antarctic station Neumayer, Atmos. Environ., 96, 11-19, https://doi.org/10.1016/j.atmosenv.2014.07.025, 2014.

Teng, X., Q. Hu, L. Zhang, J. Qi, J. Shi, H. Xie, H. Gao, and X. Yao.: Identification of major sources of

atmospheric NH3 in an urban environment in northern China during wintertime, Environ. Sci. Technol., 51, 6839−6848, 10.1021/acs.est.7b00328, 2017.

Tian, H., J. Gao, L. Lu, D. Zhao, K. Cheng, and P. Qiu.: Temporal trends and spatial variation characteristics of hazardous air pollutant emission inventory from municipal solid waste incineration in China, Environ. Sci. Technol., 46(18), 10364-10371, 10.1021/es302343s, 2012.

Tian, H., K. Liu, J. Hao, Y. Wang, J. Gao, P. Qiu, and C. Zhu.: Nitrogen oxides emissions from thermal power plants in China: Current status and future predictions, Environ. Sci. Technol., 47(19), 11350-11357, 10.1021/es402202d, 2013.

Tian, H., K. Liu, J. Zhou, L. Lu, J. Hao, P. Qiu, J. Gao, C. Zhu, K. Wang, and S. Hua.: Atmospheric Emission Inventory of Hazardous Trace Elements from China's Coal-Fired Power Plants Temporal Trends and Spatial Variation Characteristics, Environ. Sci. Technol., 48(6), 3575-3582, 10.1021/es404730j, 2014.

Turekian, K. K.: Oceans, Prentice-Hall, New Jersey, United States, 1968.

Tsai, Y.I., Hsieh, L.Y., Kuo, S.C., Chen, C.L., Wu, P.L.: Seasonal and rainfall-type variations in inorganic ions and dicarboxylic acids and acidity of wet deposition samples collected from subtropical East Asia. Atmos. Environ. 45, 3535-3547, https://doi.org/10.1016/j.atmosenv.2011.04.001, 2011.

Vašát, R., L. Pavlů, L. Borůvka, V. Tejnecký, and A. Nikodem.: Modelling the impact of acid deposition on forest soils in north Bohemian Mountains with two dynamic models: The Very Simple Dynamic Model (VSD) and the Model of Acidification of Groundwater in Catchments (MAGIC), Soil Water Res., 10(1), 10-18, 2015.

Velthof, G., J. Lesschen, J. Webb, S. Pietrzak, Z. Miatkowski, M. Pinto, J. Kros, and O. Oenema.: The impact of the Nitrates Directive on nitrogen emissions from agriculture in the EU-27 during 2000-2008,

Sci. Total Environ., 468, 1225-1233, https://doi.org/10.1016/j.scitotenv.2013.04.058, 2014.

Wang, F.Y., Liu, R.J., Lin, X.G., Zhou, J.M.: Arbuscular mycorrhizal status of wild plants in saline-alkaline soils of the Yellow River Delta. Mycorrhiza 14, 133-137, 2004.

Wang, H., J. An, M. Cheng, L. Shen, B. Zhu, Y. Li, Y. Wang, Q. Duan, A. Sullivan, and L. Xia.: One year online measurements of water-soluble ions at the industrially polluted town of Nanjing, China: Sources, seasonal and diurnal variations, Chemosphere, 148, 526-536, https://doi.org/10.1016/j.chemosphere.2016.01.066, 2016a.

Wang, J., Qiu, Y., He, S.T., Liu, N., Xiao, C.Y., Liu, L.X.: Investigating the driving forces of NOx generation from energy consumption in China. Atmos. Chem. Physics., 184, 836-846, 2018.

Wang, K., H. Tian, S. Hua, C. Zhu, J. Gao, Y. Xue, J. Hao, Y. Wang, and J. Zhou.: A comprehensive emission inventory of multiple air pollutants from iron and steel industry in China: temporal trends and spatial variation characteristics, Sci. Total Environ., 559, 7-14, https://doi.org/10.1016/j.scitotenv.2016.03.125, 2016b.

Wang, S., K. Luo, X. Wang, and Y. Sun (2016c), Estimate of sulfur, arsenic, mercury, fluorine emissions due to spontaneous combustion of coal gangue: An important part of Chinese emission inventories, Environ. Pollut., 209, https://doi.org/10.1016/j.envpol.2015.11.026, 107-113.

Wang, Y., R. Wang, J. Ming, G. Liu, T. Chen, X. Liu, H. Liu, Y. Zhen, and G. Cheng (2016d), Effects of dust storm events on weekly clinic visits related to pulmonary tuberculosis disease in Minqin, China, Atmos. Environ., 127, https://doi.org/10.1016/j.atmosenv.2015.12.041, 205-212.

Wang, Q.: Effects of urbanisation on energy consumption in China, Energ. Policy, 65, 332-339, 2014.

Wang, Q., G. Zhuang, K. Huang, T. Liu, C. Deng, J. Xu, Y. Lin, Z. Guo, Y. Chen, and Q. Fu.: Probing the severe haze pollution in three typical regions of China: Characteristics, sources and regional impacts,

Atmos. Environ., 120, 76-88, https://doi.org/10.1016/j.atmosenv.2015.08.076, 2015a.

Wang, X., W. Pu, J. Shi, J. Bi, T. Zhou, X. Zhang, and Y. Ren.: A comparison of the physical and optical properties of anthropogenic air pollutants and mineral dust over Northwest China, Acta Meteorol Sin., 29(2), 180-200, 2015b.

Wang, Y., Y. Xue, H. Tian, J. Gao, Y. Chen, C. Zhu, H. Liu, K. Wang, S. Hua, and S. Liu.: Effectiveness of temporary control measures for lowering $PM_{2.5}$ pollution in Beijing and the implications, Atmos. Environ., 157, 75-83, https://doi.org/10.1016/j.atmosenv.2017.03.017, 2017.

Wei, F. S., Chen, J. S., Wu, Y. Y., Zheng, C.J.: The study of background value in soil across China. Environ. Sci., 12, 12-20, 1991 (in Chinese).

Wei, F.S., Yang, G.Z., Jiang, D.Z., Liu, Z.H., Sun, B.M.: The basic statistics and characteristics of soil elements in China. Environ. Moni. China., 7, 1-6, 1991 (in Chinese).

Wu, J., Li, P., Qian, H., Duan, Z., Zhang, X.: Using correlation and multivariate statistical analysis to identify hydrogeochemical processes affecting the major ion chemistry of waters: a case study in Laoheba phosphorite mine in Sichuan, China, Arab. J. Geosci., 7, 3973–3982, 2014.

Wu, Q., and G. Han.: Sulfur isotope and chemical composition of the precipitation at the Three Gorges Reservoir, Atmos. Res., 155, 130-140, https://doi.org/10.1016/j.atmosres.2014.11.020, 2015.

Wu, J., G. Liang, D. Hui, Q. Deng, X. Xiong, Q. Qiu, J. Liu, G. Chu, G. Zhou, and D. Zhang.: Prolonged acid rain facilitates soil organic carbon accumulation in a mature forest in Southern China, Sci. Total Environ., 544, 94-102, https://doi.org/10.1016/j.scitotenv.2015.11.025, 2016a.

Wu, X.M., Wu, Y., Zhang, S.J., Liu, H., Fu, L.X., Hao, J.M.: Assessment of vehicle emission programs in China during 1998-2013: achievement, challenges and implications, Environ. Pollut., 214, 556-567, https://doi.org/10.1016/j.envpol.2016.04.042, 2016b.

Xiao, H.W., H.-Y. Xiao, A.-M. Long, Y.-L. Wang, and C.-Q. Liu.: Sources and meteorological factors that control seasonal variation of δ ^{34}S values in precipitation, Atmos. Res., 149, 154-165, https://doi.org/10.1016/j.atmosres.2014.06.003, 2014.

Xing, J., J. Song, H. Yuan, X. Li, N. Li, L. Duan, X. Kang, and Q. Wang.: Fluxes, seasonal patterns and sources of various nutrient species (nitrogen, phosphorus and silicon) in atmospheric wet deposition and their ecological effects on Jiaozhou Bay, North China, Sci. Total Environ., 576, 617-627, https://doi.org/10.1016/j.scitotenv.2016.10.134, 2017.

Xu, P., Y. Liao, Y. Lin, C. Zhao, C. Yan, M. Cao, G. Wang, and S. Luan.: High-resolution inventory of ammonia emissions from agricultural fertilizer in China from 1978 to 2008, Atmos. Chem. Phys., 16(3), 1207-1218, https://doi.org/10.5194/acp-16-1207-2016, 2016.

Xu, W., X. Luo, Y. Pan, L. Zhang, A. Tang, J. Shen, Y. Zhang, K. Li, Q. Wu, and D. Yang.: Quantifying atmospheric nitrogen deposition through a nationwide monitoring network across China, Atmos. Chem. Phys., 15(21), 12345-12360, https://doi.org/10.5194/acp-15-12345-2015, 2015.

Yan, W., E. Mayorga, X. Li, S. P. Seitzinger, and A. Bouwman.: Increasing anthropogenic nitrogen inputs and riverine DIN exports from the Changjiang River basin under changing human pressures, Global Biogeochem. Cy., 24(4), https://doi.org/10.1029/2009GB003575, 2010.

Yang, K., J. Zhu, J. Gu, L. Yu, and Z. Wang.: Changes in soil phosphorus fractions after 9 years of continuous nitrogen addition in a Larix gmelinii plantation, Ann. For. Sci., 72(4), 435-442, 2015.

Yang, X., Shen, S.H., Ying, F., He, Q., Ali, M., Huo, W., Liu, X.C.: Spatial and temporal variations of blowing dust events in the Taklimakan Desert, Theor. Appl. Climato., 125, 669-677, 2016a.

Yang, Y., R. Zhou, Y. Yan, Y. Yu, J. Liu, Z. Du, and D. Wu.: Seasonal variations and size distributions of water-soluble ions of atmospheric particulate matter at Shigatse, Tibetan Plateau, Chemosphere, 145,

560-567, https://doi.org/10.1016/j.chemosphere.2015.11.065, 2016b.

Yang, X., S. Wang, W. Zhang, and J. Yu.: Are the temporal variation and spatial variation of ambient SO_2 concentrations determined by different factors? J. Clean Prod., 167, 824-836, https://doi.org/10.1016/j.jclepro.2017.08.215, 2017.

Yu, H. L., He, N. P., Wang, Q. F., Zhu, J. X., Xu, L., Zhu, Z. L., Yu, G. R.: Wet acid deposition in Chinese natural and agricultural ecosystems: Evidence from national-scale monitoring, J. Geophys. Res. Atmos., 121, 1-11, https://doi.org/10.1002/2015JD024441, 2016.

Yu, H., N. He, Q. Wang, J. Zhu, Y. Gao, Y. Zhang, Y. Jia, and G. Yu.: Development of atmospheric acid deposition in China from the 1990s to the 2010s, Environ. Pollut., 231, 182-190, https://doi.org/10.1016/j.envpol.2017.08.014, 2017a.

Yu, Y., S. Zhao, B. Wang, P. Fu, and J. He.: Pollution Characteristics Revealed by Size Distribution Properties of Aerosol Particles at Urban and Suburban Sites, Northwest China, Aerosol Air Qual Re., 17(7), 1784-1797, 10.4209/aaqr.2016.07.0330, 2017b.

Zhai, P.M., Li, X.Y.: On climate background of duststorms over northern China, Acta Geographica Sinica, 58, 2003 (in Chinese).

Zhan, Y., Luo, Y.Z., Deng, X.F., Zhang, K.S., Zhang, M.H., Grieneisen, M.L., Di, B.F., 2018. Satellited-based estimates of daily NO_2 exposure in China using hybrid random forest and spatiotemporal Kriging model. Environ. Sci. Tech. 52, 4180-4189, 2018.

Zhang, S.L., Yang, G.Y.: Changes of background values of inorganic elements in soils of gunagdong province, Soils, 1009-1014, 2012 (in Chinese).

Zhang, T., J. Cao, X. Tie, Z. Shen, S. Liu, H. Ding, Y. Han, G. Wang, K. Ho, and J. Qiang.: Water-soluble ions in atmospheric aerosols measured in Xi'an, China: seasonal variations and sources, Atmos Res.,

102(1), 110-119, https://doi.org/10.1016/j.atmosres.2011.06.014, 2011.

Zhang, X.-X., B. Sharratt, X. Chen, Z.-F. Wang, L.-Y. Liu, Y.-H. Guo, J. Li, H.-S. Chen, and W.-Y. Yang.: Dust deposition and ambient PM_{10} concentration in northwest China: spatial and temporal variability, Atmos. Chem. Phys., 17(3), 1699-1711, https://doi.org/10.5194/acp-17-1699-2017, 2017a.

Zhang, Y., J. Wei, A. Tang, A. Zheng, Z. Shao, and X. Liu.: Chemical Characteristics of $PM_{2.5}$ during 2015 Spring Festival in Beijing, China, Aerosol Air Qual. Re., 17(5), 1169-1180, 10.4209/aaqr.2016.08.0338, 2017b.

Zhang, Z., J. Gao, L. Zhang, H. Wang, J. Tao, X. Qiu, F. Chai, Y. Li, and S. Wang.: Observations of biomass burning tracers in $PM_{2.5}$ at two megacities in North China during 2014 APEC summit, Atmos. Environ., 169, 54-64, https://doi.org/10.1016/j.atmosenv.2017.09.011, 2017c.

Zhang, X., F. Chai, S. Wang, X. Sun, and M. Han.: Research progress of acid precipitation in China, Res. Environ. Sci., 23(5), 527-532, 2010 (in Chinese).

Zhang, Y.Y., Liu, J.F., Mu, Y.J., Pei, S.W., Lun, X.X., Chai, F.H.: Emissions of nitrous oxide, nitrogen oxides and ammonia from a maize field in the North China Plain, Atmos. Environ., 45, 2956-2961, https://doi.org/10.1016/j.atmosenv.2010.10.052, 2011.

Zhang, Y., W. Huang, T. Cai, D. Fang, Y. Wang, J. Song, M. Hu, and Y. Zhang.: Concentrations and chemical compositions of fine particles ($PM_{2.5}$) during haze and non-haze days in Beijing, Atmos. Res., 174, 62-69, https://doi.org/10.1016/j.atmosres.2016.02.003, 2016.

Zhao, C., and K. Luo.: Sulfur, arsenic, fluorine and mercury emissions resulting from coal-washing byproducts: A critical component of China's emission inventory, Atmos. Environ., 152, 270-278, https://doi.org/10.1016/j.atmosenv.2016.12.001, 2017.

Zhao, J., F. Zhang, Y. Xu, and J. Chen.: Characterization of water-soluble inorganic ions in size-

segregated aerosols in coastal city, Xiamen, Atmos. Res., 99(3), 546-562, https://doi.org/10.1016/j.atmosres.2010.12.017, 2011.

Zhao, M., S. Wang, J. Tan, Y. Hua, D. Wu, and J. Hao.: Variation of urban atmospheric ammonia pollution and its relation with $PM_{2.5}$ chemical property in winter of Beijing, China, Aerosol Air Qual. Res., 16(6), 1378-1389, 10.4209/aaqr.2015.12.0699, 2016.

Zheng, B., H. Huo, Q. Zhang, Z. Yao, X. Wang, X. Yang, H. Liu, and K. He.: High-resolution mapping of vehicle emissions in China in 2008, Atmos. Chem. Phys., 9787, https://doi.org/10.5194/acp-14-9787-2014, 2014.

Zhou, Y., Y. Zhao, P. Mao, Q. Zhang, J. Zhang, L. Qiu, and Y. Yang.: Development of a high-resolution emission inventory and its evaluation and application through air quality modeling for Jiangsu Province, China, Atmos. Chem. Phys., 17(1), 211-233, https://doi.org/10.5194/acp-17-211-2017, 2017a.

Zhou, Y., Xing, X.F., Lang, J.L., Chen, D.S., Cheng, S.Y., Wei, L., Wei, X., Liu, C.: A comprehensive biomass burning emission inventory with highspatial and temporal resolution in China, Atmos. Chem. Phys., 17, 2839-2864, https://doi.org/10.5194/acp-17-2839-2017, 2017b.

Figure and table caption

Fig. 1 The spatial distribution of 320 cities and five ecological regions.

Fig. 2 The inter-annual and seasonal variation of pH and EC of the precipitation in China.

Fig. 3 The spatial distribution of pH and EC of the precipitation in China.

Fig. 4 The temporal variation of water-soluble ions in the precipitation.

Fig. 5 The spatial variation of NO_3^-, NH_4^+, and SO_4^{2-} in the precipitation.

Fig. 6 The spatial distribution of Ca^{2+}, Cl^-, F^-, K^+, Mg^{2+}, and Na^+ in the precipitation.

Fig. 7 The triangular diagrams of NF for main alkaline ions.

Fig. 8 The EF_{sea} and EF_{soil} of NO_3^-, SO_4^{2-}, and NH_4^+.

Fig. 9 The spatial variation of SSF, CF, and AF for NO_3^-, NH_4^+, and SO_4^{2-} in the precipitation.

Fig. 10 The seasonal difference of contribution ratios of anthropogenic source, crustal source, and, sea source.

Fig. 11 The local regression coefficient of influential factors for the NO_3^-, NH_4^+, and SO_4^{2-}.

Tab. 1 The comparison of physicochemical properties and chemical composition in the precipitation.

Tab. 2 The mean enrichment factor relative to sea and soil, and the source contribution (%) of major ions in China (SSF denotes sea salt fraction, CF represents the crustal source, AF indicates the anthropogenic fraction).

Tab. 3 The loading matrix of precipitation in four seasons of China.

Tab. 4 The results of stepwise regression method.

Fig. 1

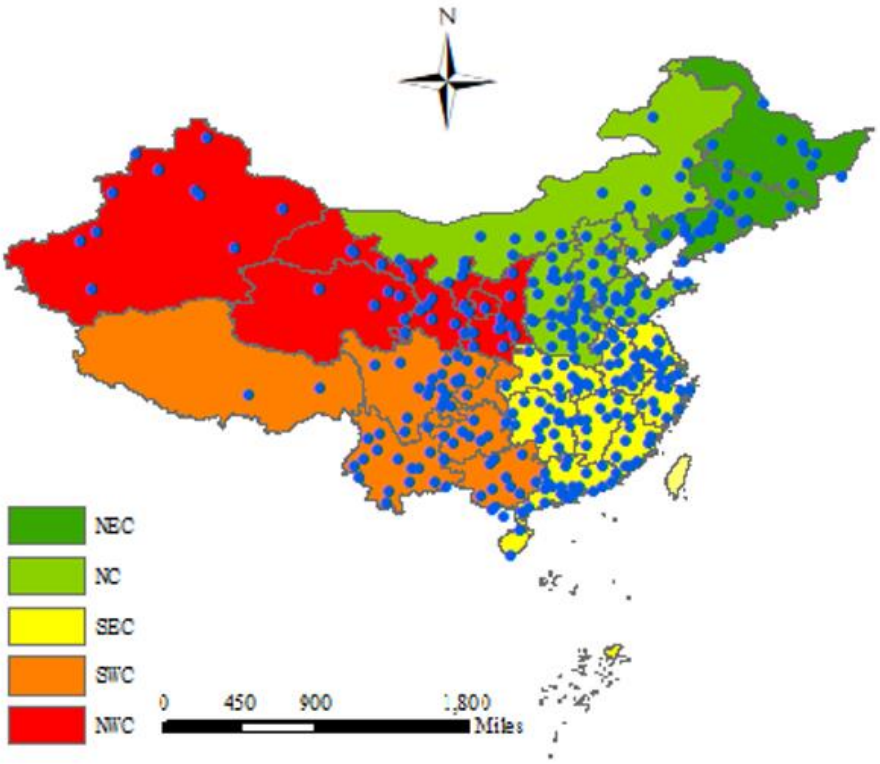

Fig. 2

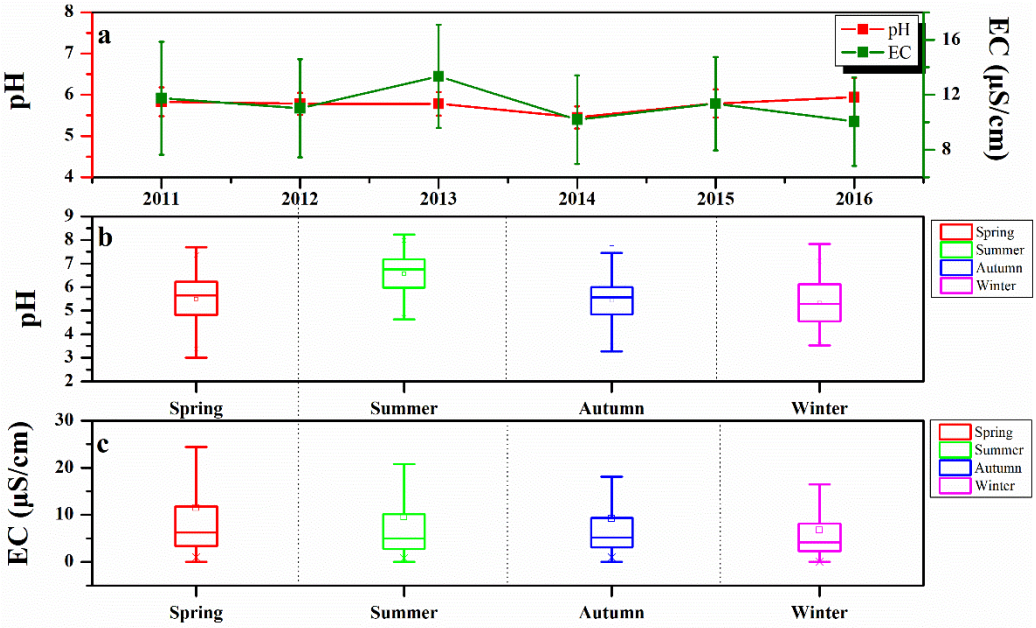
a
pH
EC
pH
EC (µS/cm)
2011
2012
2013
2014
2015
2016
b
pH
Spring
Summer
Autumn
Winter
c
EC (µS/cm)
Spring
Summer
Autumn
Winter

Fig. 3

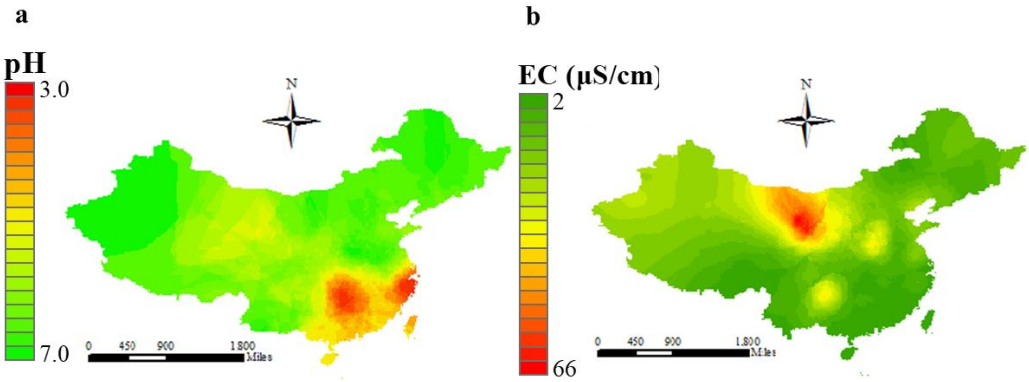
a
pH
3.0
7.0
N
0 450 900 1,800
Miles
b
EC (μS/cm)
2
66
N
0 450 900 1,800
Miles

Fig. 4

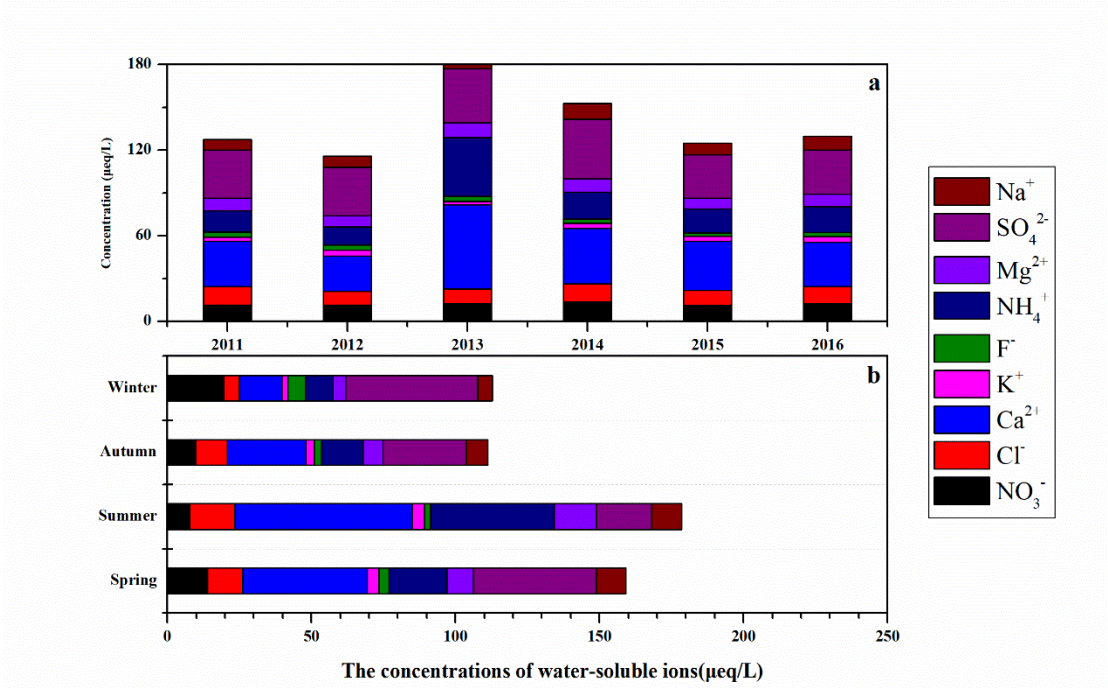
a
b
Concentration (ueq/L)
180
120
60
0
2011
2012
2013
2014
2015
2016
Winter
Autumn
Summer
Spring
0
50
100
150
200
250
The concentrations of water-soluble ions(μeq/L)
Na+
SO4 2-
Mg2+
NH4 +
F-
K+
Ca2+
Cl-
NO3 -

Fig. 5

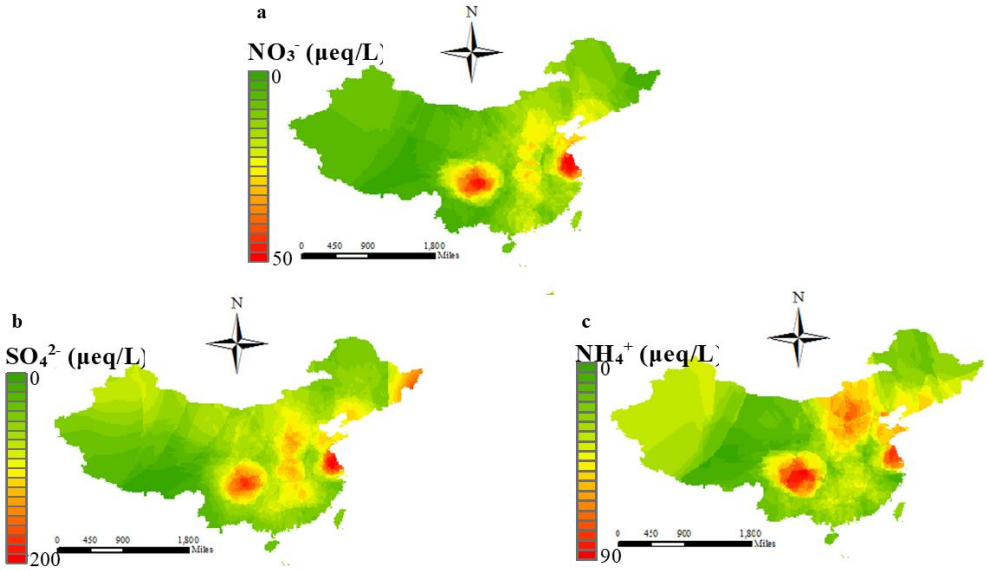
a
NO_3^- (μeq/L)
0
50
N
0 450 900 1,800
Miles
b
SO_4^{2-} (μeq/L)
0
200
N
0 450 900 1,800
Miles
c
NH_4^+ (μeq/L)
0
90
N
0 450 900 1,800
Miles

Fig. 6

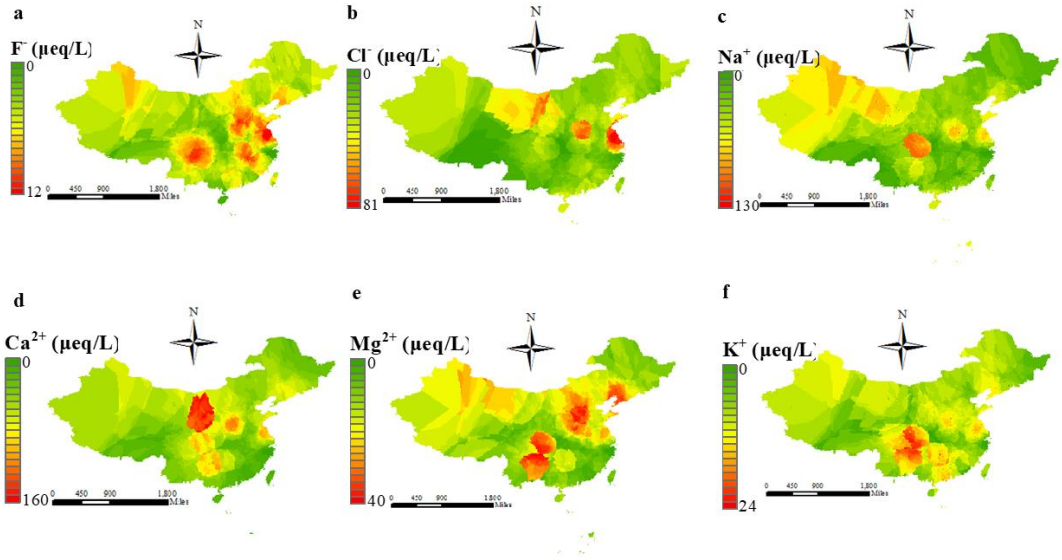
a
F⁻ (μeq/L)
0
12
b
Cl⁻ (μeq/L)
0
81
c
Na⁺ (μeq/L)
0
130
d
Ca²⁺ (μeq/L)
0
160
e
Mg²⁺ (μeq/L)
0
40
f
K⁺ (μeq/L)
0
24
N
0 450 900 1,800
Miles

Fig. 7

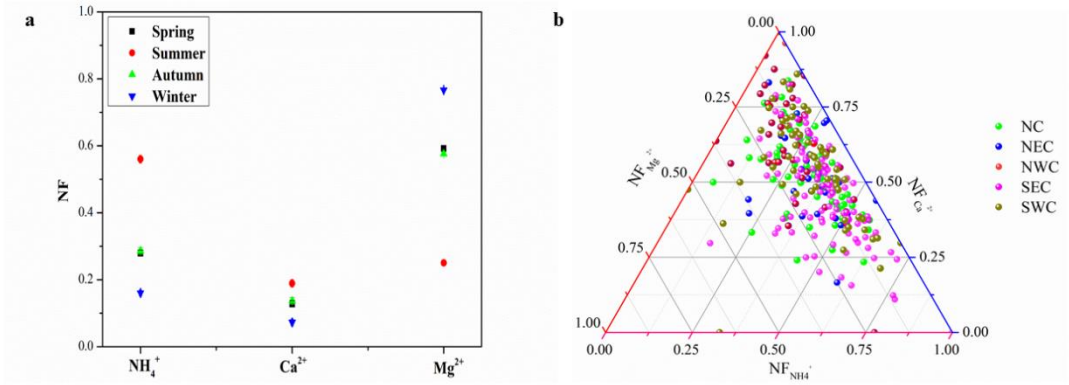
a
Spring
Summer
Autumn
Winter
NF
1.0
0.8
0.6
0.4
0.2
0.0
NH4+
Ca2+
Mg2+
b
0.00
1.00
0.25
0.75
0.50
0.50
0.75
0.25
1.00
0.00
0.00
0.25
0.50
0.75
1.00
NF Mg2+
NF Ca2+
NF NH4+
NC
NEC
NWC
SEC
SWC

Fig. 8

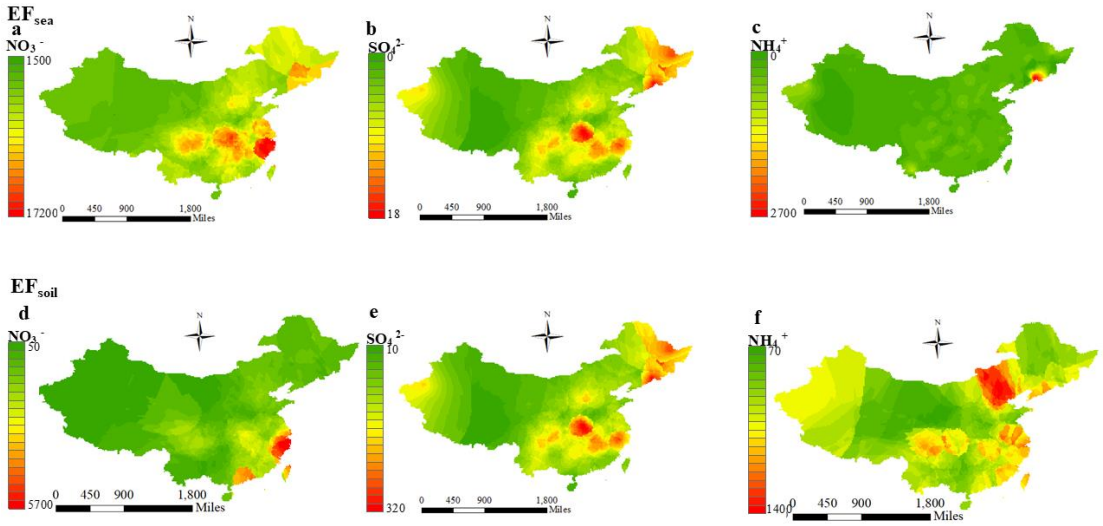
EF sea
a
NO3 -
1500
17200
0 450 900 1,800
Miles
b
SO4 2-
0
18
0 450 900 1,800
Miles
c
NH4 +
0
2700
0 450 900 1,800
Miles
EF soil
d
NO3 -
50
5700
0 450 900 1,800
Miles
e
SO4 2-
10
320
0 450 900 1,800
Miles
f
NH4 +
70
1400
0 450 900 1,800
Miles

Fig. 9

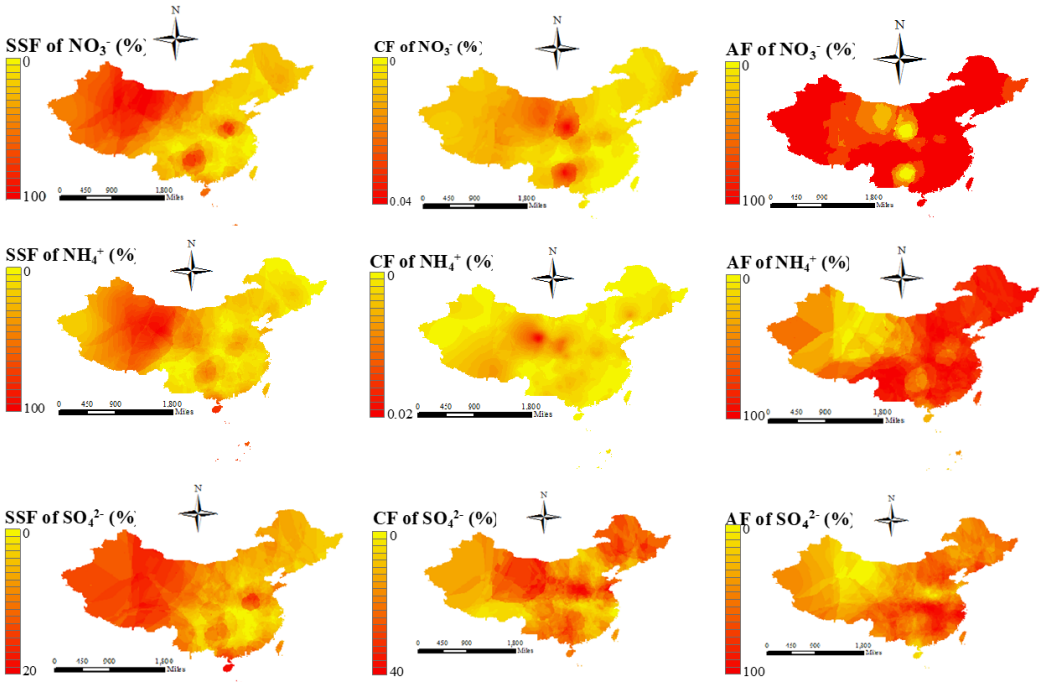
SSF of NO_3^- (%)
0
100
CF of NO_3^- (%)
0
0.04
AF of NO_3^- (%)
0
100
SSF of NH_4^+ (%)
0
100
CF of NH_4^+ (%)
0
0.02
AF of NH_4^+ (%)
0
100
SSF of SO_4^{2-} (%)
0
20
CF of SO_4^{2-} (%)
0
40
AF of SO_4^{2-} (%)
0
100
N
0 450 900 1,800
Miles

Fig. 10

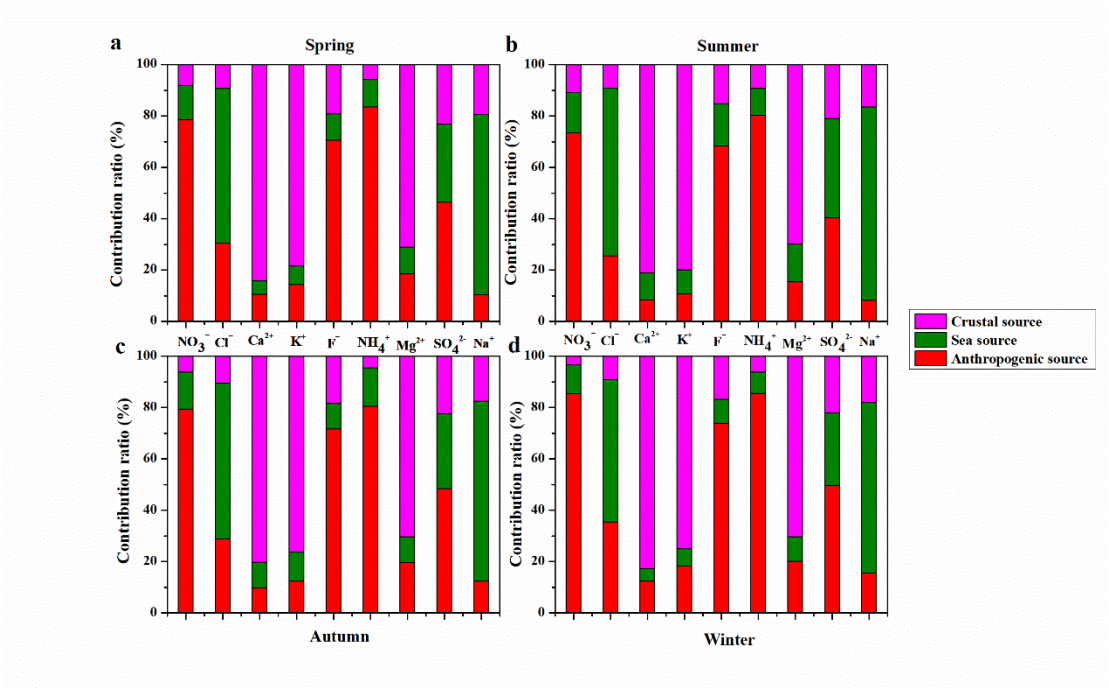
a
Spring
b
Summer
c
Autumn
d
Winter
Contribution ratio (%)
0
20
40
60
80
100
NO3- Cl- Ca2+ K+ F- NH4+ Mg2+ SO4 2- Na+
Crustal source
Sea source
Anthropogenic source

Fig. 11

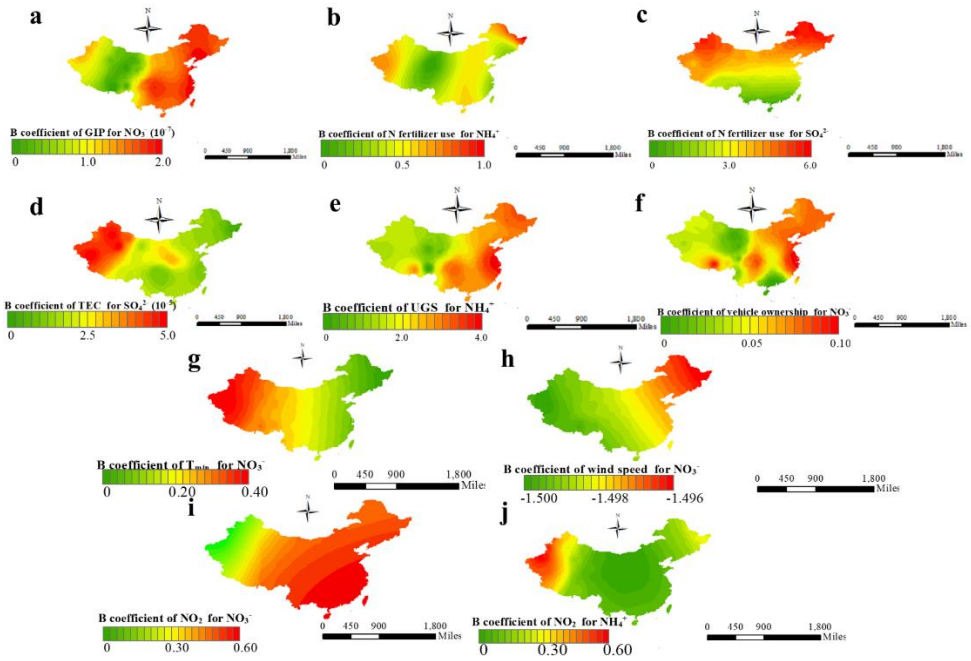
a
B coefficient of GIP for NO3- (10-7)
0
1.0
2.0
b
B coefficient of N fertilizer use for NH4+
0
0.5
1.0
c
B coefficient of N fertilizer use for SO42-
0
3.0
6.0
d
B coefficient of TEC for SO42- (10-5)
0
2.5
5.0
e
B coefficient of UGS for NH4+
0
2.0
4.0
f
B coefficient of vehicle ownership for NO3-
0
0.05
0.10
g
B coefficient of Tmin for NO3-
0
0.20
0.40
h
B coefficient of wind speed for NO3-
-1.500
-1.498
-1.496
i
B coefficient of NO2 for NO3-
0
0.30
0.60
j
B coefficient of NO2 for NH4+
0
0.30
0.60
0 450 900 1,800 Miles

Tab. 1

	pH	EC	NO_3^-	Cl^-	Ca^{2+}	K^+	F^-	NH_4^+	Mg^{2+}	SO_4^{2-}	Na^+	Year	References
Beijing	5.68	9.89	15.13	6.62	26.27	1.80	2.24	45.33	5.51	31.28	3.39	2011-	This study
Zhengzhou	6.09	26.44	37.10	72.45	109.23	8.25	5.80	23.82	20.54	25.80	6.40	2011-	This study
Harbin	6.13	7.41	9.87	20.71	21.98	5.02	5.03	11.96	9.55	28.76	22.00	2011-	This study
Shenyang	5.76	8.40	24.52	15.90	75.32	2.59	4.32	40.68	22.68	57.57	16.88	2011-	This study
Qingdao	5.32	16.53	5.25	5.79	28.18	2.07	1.34	9.28	9.80	10.96	25.30	2011-	This study
Shanghai	4.39	2.50	40.06	4.15	19.09	1.07	1.45	17.48	4.71	29.13	20.36	2011-	This study
Wuhan	4.68	2.66	11.61	2.12	13.55	0.76	1.07	9.38	2.63	27.93	1.28	2011-	This study
Guangzhou	4.98	2.84	26.74	19.38	41.60	9.42	3.93	13.58	8.33	35.76	9.57	2011-	This study
Chengdu	4.89	6.03	48.08	22.13	44.42	12.60	9.21	65.19	8.23	77.16	15.06	2011-	This study
Lhasa	5.21	4.51	0.50	1.65	7.66	0.48	0.94	0.91	1.28	1.44	1.62	2011-	This study
Urumqi	6.13	13.41	16.87	30.38	115.24	4.76	2.02	73.76	19.41	56.76	28.87	2011-	This study
Lanzhou	5.05	58.06	16.19	4.93	51.84	1.24	1.57	3.05	8.17	33.30	10.87	2011-	This study
Jiuzhaigou	5.95	15.70	9.10	44.10	55.80	34.80	0.86	18.40	5.60	15.90	12.60	2015-	Qiao et al. (2018)
Yulong	5.94	10.30	4.00	1.96	37.7	2.46	1.20	13.20	5.68	28.30	3.72	2012	Niu et al. (2014)
Nam Co	6.59	19.70	10.00	19.20	301	14.50	-	18.10	7.43	15.50	15.40	2005	Li et al. (2007)
Southern	-	-	20.97	31.06	46.68	11.14	-	58.57	22.55	45.97	56.41	2005-	Tsai et al. (2011)
Petra,	6.80	160	35.70	80.60	163.10	26.30	-	18.40	62.30	53.20	75.60	2002-	Al-Khashman et al. (2005)
Tokyo,	4.52	-	30.50	55.20	24.90	2.90	-	40.4	11.5	50.2	37.0	1990-	Okuda et al. (2005)
Guaíba,	5.92	10.8	4.00	13.80	21.50	5.81	5.90	38.90	8.85	23.10	15.10	2002	Migliavacca et al. (2005)
Sao Paulo,	-	-	15.60	0.90	5.50	3.70	-	27.90	1.70	8.60	3.60	2000	Fornaro and Gutz (2003).
Singapore	-	-	16.80	22.10	21.7	3.96	-	17.3	7.46	58.7	31.1	1997-	Balasubramanian et al. (2001)
Newark,	-	-	14.40	10.70	6.00	1.30	-	24.40	3.30	38.10	10.90	2006-	Song and Gao (2009)
Patras,	5.16	--	19.40	114.30	98.50	6.60	--	16.30	30.40	46.10	90.20	2000-	Glavas and Moschonas (2002)
Sardinia,	5.18	--	29	322	70	17	--	25	77	90	252	1992-	Le Bolloch and Guerzoni (1995)
Adirondack,	4.50	--	22.60	2.14	3.59	0.33	--	10.50	0.99	36.90	1.61	1988-	Ito et al. (2002)

Tab. 2

	EF_{sea}	EF_{soil}	SSF	CF	AF
NO_3^-	3507.49	59.36	0	0.02	99.98
Cl-	1.13	169.88	88.31	0.59	11.10
Ca^{2+}	231.56	1.00	0.06	99.94	0
K^+	16.16	0.83	4.88	95.12	0
F^-	5864.28	9.96	0.02	10.04	89.94
NH_4^+	10.51	86.31	0.10	0.01	99.89
Mg^{2+}	10.18	0.55	2.94	97.06	0
SO_4^{2-}	7.22	5.13	13.85	19.50	66.65
Na^+	1.00	1.83	64.66	35.34	0

Tab. 3

Season	Variable	F1	F2	F3
Overall	NO_3^-	**0.71**	0.24	0.45
	Cl^-	0.43	**0.64**	-0.12
	Ca^{2+}	0.42	-0.22	**0.75**
	K^+	0.39	0.18	**0.72**
	F^-	**0.68**	-0.20	0.45
	NH_4^+	**0.74**	0.35	0.13
	Mg^{2+}	-0.41	0.10	**0.66**
	SO_4^{2-}	**0.63**	0.23	0.14
	Na^+	-0.02	**0.65**	0.45
Spring	NO_3^-	**0.76**	0.11	-0.32
	Cl^-	-0.33	**0.59**	0.26
	Ca^{2+}	0.32	-0.16	**0.80**
	K^+	-0.36	0.06	**0.78**
	F^-	**0.70**	-0.10	0.20
	NH_4^+	**0.68**	0.29	-0.46
	Mg^{2+}	-0.38	0.42	**0.69**
	SO_4^{2-}	**0.77**	0.31	0.22
	Na^+	-0.04	**0.72**	0.46
Summer	NO_3^-	**0.63**	0.24	-0.33
	Cl^-	0.42	**0.66**	-0.38
	Ca^{2+}	0.44	-0.26	**0.85**
	K^+	-0.37	0.19	**0.70**
	F^-	**0.54**	-0.32	0.48
	NH_4^+	**0.59**	0.33	-0.47
	Mg^{2+}	0.32	-0.38	**0.60**
	SO_4^{2-}	**0.56**	0.36	0.34
	Na^+	-0.09	**0.75**	0.49
Autumn	NO_3^-	**0.73**	-0.14	0.38
	Cl^-	-0.39	**0.62**	0.29
	Ca^{2+}	0.32	-0.16	**0.80**
	K^+	0.45	-0.09	**0.68**
	F^-	**0.68**	-0.15	0.28

	NH_4^+	**0.69**	0.42	-0.45
	Mg^{2+}	-0.29	0.32	**0.71**
	SO_4^{2-}	**0.68**	-0.29	0.23
	Na^+	-0.14	**0.69**	-0.37
Winter	NO_3^-	**0.79**	0.23	-0.36
	Cl^-	-0.38	**0.49**	0.29
	Ca^{2+}	0.39	-0.35	**0.65**
	K^+	-0.39	0.08	**0.72**
	F^-	**0.75**	0.08	-0.24
	NH_4^+	**0.73**	0.26	-0.42
	Mg^{2+}	0.35	-0.49	**0.75**
	SO_4^{2-}	**0.79**	0.22	0.36
	Na^+	-0.16	**0.54**	0.33

Tab. 4

Dependent variables	Independent variables	Partial regression coefficients	R^2	t value	p value
NO_3^-	GIP	8.42×10^{-8}	0.62	4.03	0.00
	Vehicle ownership	0.03		-2.39	0.01
	NO_2	0.34		4.29	0.00
	T_{min}	0.15		1.34	0.02
	Wind speed	-1.49		-1.69	0.03
Cl^-	Dust days	0.12	0.52	2.14	0.04
Ca^{2+}	PM_{10}	0.36	0.56	3.26	0.00
	Dust days	132.74		2.99	0.00
K^+	Dust days	2.09	0.49	2.03	0.02
F^-	GIP	0.54×10^{-7}	0.50	2.31	0.02
NH_4^+	N fertilizer use	0.14	0.48	2.46	0.02
	UGS	1.33×10^{-4}		1.79	0.04
	NO_2	0.25		1.98	0.03
Mg^{2+}	Dust days	2.36	0.43	1.65	0.05
SO_4^{2-}	TEC	2.80×10^{-5}	0.64	3.07	0.00
	N fertilizer use	3.36		3.59	0.00
Na^+	Dust days	2.46	0.46	1.69	0.04